NATIONAL TRANSPORTATION SAFETY BOARD
Office of Research and Engineering
Materials Laboratory Division
Washington, D.C. 20594

May 17, 2011

MATERIALS LABORATORY FACTUAL REPORT Report No. 11-056

A. ACCIDENT INFORMATION

Place	:	San Bruno, California
Date	:	September 9, 2010
Vehicle	:	Pacific Gas & Electric Natural Gas Transmission Pipeline
NTSB No.	:	DCA10MP008
Investigator	:	Ravindra Chhatre, RPH-20

B. COMPONENTS EXAMINED

Three pieces of 30-inch diameter pipe from Line 132, Segment 180, located at the intersection of Earl Avenue and Glenview Drive, San Bruno, California, with the following lengths:

1) 12 foot 4 inch
2) 27 foot 8 inch
3) 15 foot 9 inch

C. DETAILS OF THE EXAMINATION

These three pieces of pipe were previously examined and much of the findings previously documented. The Metallurgical Group Chairman's Factual Report (Materials Laboratory Report 10-119) provided information on the as-received condition of the pipe pieces, non-destructive testing, fractographic determination of the initiation site, and metallography of the longitudinal seams (NTSB, 2011a). The Metallurgical Group Chairman's Factual Report—Addendum 1 (Materials Laboratory Report 11-005) provided chemical composition data, tensile test data, rolling direction data, and metallographic characterization of girth welds on the pipe pieces (NTSB, 2011b).

The pipeline was constructed as illustrated by the schematic in Figure 1. For convenience, pups 1–6 are abbreviated and numbered P1, P2, and so on through P6 from south to north and the girth welds between the pups are numbered C1, C2, and so on through C7 from south to north. References to the length of pipe south of pup 1 are abbreviated LS and references to the length of pipe north of pup 6 are abbreviated LN.

This report describes additional fractography on the longitudinal seams on P1–P3, weld depth measurements on P2 and P3, pipe circumference measurements, characterization of weld microstructure, and microhardness testing of the longitudinal seam welds on each length of pipe.

C.1. FRACTOGRAPHY, WELD DEPTH, AND PIPE CIRCUMFERENCE

The P1 longitudinal seam fracture was previously characterized on the counterclockwise (CCW)[1] fracture face as was the P2 longitudinal seam fracture at the upstream end near girth weld C2, where P2 joined P1 (NTSB, 2001a). This section provides fractographic documentation of the P1 longitudinal fracture on the clockwise (CW) fracture face, the longitudinal fracture at the downstream end of the P2 longitudinal seam near girth weld C3, and the P3 longitudinal seam fractured by hand in the lab.

The CW fracture face of the P1 longitudinal seam showed the same features that were previously documented on the CCW face, except that features consistent with fatigue were identified in areas that were not interpretable on the CCW face. A macrophotograph of the CW fracture face of the P1 longitudinal seam at the initiation site is shown in Figure 2. The image on the bottom has two yellow dashed lines superimposed on it that bound areas where features consistent with fatigue were observed by scanning electron microscope (SEM). SEM micrographs taken at various locations inside the area bounded by the yellow-dashed lines are shown in Figures 3 through 5. Features consistent with striations are indicated in each of the figures.

The weld depth, intact wall thickness after crack progression by overstress, and intact wall thickness after crack progression by overstress and fatigue, as determined by SEM, were measured at approximately 0.10-inch intervals along the initiation site . An example of each measurement, referenced with respect to the outer surface, is indicated by arrows a, b, and c in Figure 2, respectively, as is the 0.0 inch datum, located at the upstream end of the crack. The thickness data are shown graphically in Figure 6 and a table of measured values is in Appendix A. The average wall thickness was 0.165 inch ± 0.008 inch. Based on the datum in Figure 6, the wall thickness deviated from the average value by more than one standard deviation at the following locations along the longitudinal seam:

Distance from datum	Wall thickness
0.0 inch	0.151 inch
1.0 inch–1.2 inch	0.180 inch
1.8 inch–2.0 inch	0.153 inch–0.156 inch

The longitudinal position of deepest crack penetration was at 1.0 inch–1.2 inch, coinciding with the location where the initial wall thickness was at its maximum. The intact cross sectional wall area was calculated from the data in Appendix A for all three cases as a piecewise sum of trapezoidal area measurements along the seam (i.e., trapezoidal integration rule). The cross sectional area of the initial intact wall was 0.397 $inch^2$, the cross sectional area of the intact wall after crack progression by

[1] Clockwise (CW) and counterclockwise (CCW) rotations are prescribed as a circumferential rotation about the surface of the pipe when viewed along the typical direction of gas flow. The CW fracture face would then be the face that is on the CW side of the seam.

overstress was 0.267 inch^2, and the cross sectional area of the intact wall after crack progression by overstress + fatigue was 0.228 inch^2.

Occasional thumbnail-shaped features were observed along the length of the P1 longitudinal seam at the root of the weld fracture surface. Several thumbnail features on the CW side of the seam fracture, starting at the initiation site and continuing approximately 1.5 inch upstream, were examined by SEM and were found to exhibit fractographic features consistent with fatigue. Several of the thumbnail features are shown in Figure 7. The thumbnails ranged from 0.060 inch to 0.075 inch in the longitudinal direction and 0.015 inch to 0.017 inch in the through-thickness direction. One of the thumbnails, indicated by the box in Figure 7, is shown in an SEM micrograph in Figure 8. In turn, the fracture surface inside the box in Figure 8 is shown in greater detail in Figure 9. Striations, consistent with fatigue, are indicated by the rectangle.

The features of the P2 longitudinal seam fracture faces were consistent with out-of-plane shear at the upstream end near P1, transitioning to inward bending deformation downstream toward P3. Near the downstream end, two regions along the longitudinal seam exhibited light- and dark-colored fractographic features consistent with ductile fracture originating from the root of the weld. The first region extended from 29.4 inch to 32.2 inch, with respect to the upstream end of P2 (i.e., from girth weld C2), and is shown in Figure 10. The second region extended from 32.3 inch to 35.9 inch, with respect to the upstream end of P2, and is shown in Figure 11. At approximately 31 inch, with respect to the upstream end of P2, and toward the outer diameter surface, fractographic features consistent with quasi-cleavage began to appear, as shown in Figure 12. The light- and dark-colored ductile fracture regions extended from the root of the weld to the yellow-dashed lines indicated in each figure. At this location, the weld root had a scalloped morphology and the weld contained a high concentration of gas pores. The ductile fracture regions were characterized by a light-colored band near the root of the weld followed by a dark-colored band moving toward the outer diameter surface. A typical region, indicated as region A in Figure 11, was examined by SEM, as shown in Figure 13. Secondary cracking was observed at the transition between light- and dark-colored areas, as indicated in the figure. The light- and dark-colored regions were further examined at higher magnification at the regions labeled B and C, respectively. Figure 14a shows an SEM micrograph from region B at the root of the weld. The fracture surface was characterized by flattened fracture features with occasional ductile dimples observable between flattened features. Figure 14b shows an SEM micrograph from region C within the dark-colored region. The fracture surface was characterized by ductile dimples with little to no smearing.

The P3 longitudinal seam, which was still partially intact after the rupture, was fractured in the lab. A rectangular section containing the P3 longitudinal seam was cut from the pipe using a plasma cutter, leaving the first and last 4 inch of the seam attached to the pipe. Transverse cuts were typically made through the rectangular section every 5 inch or 6 inch using a band saw. The section was fractured in cantilever bending by securing one half of each section in a vice while the other half was pulled by hand at room temperature. In some instances, audible cracking could be heard and the lab-fractured regions exhibited surface features consistent with a mixture of quasi-cleavage fracture and ductile fracture. The lab-fractured surfaces were identified by their silver color, typical of a fresh fracture. An example can be seen in Figure 15 adjacent to the outer diameter surface.

The appearance of the P3 longitudinal seam was consistent with cracking of the seam prior to the lab fracture. The prior fracture surface exhibited primarily quasi-cleavage fracture from the root of the weld. A typical location, examined by SEM, is shown in Figure 16. Certain regions exhibited features consistent with ductile fracture or features consistent with corrosion starting at the root of the weld, as described below.

Some sections along the seam were covered with a discontinuous orange-colored layer, consistent with rust. Regions of the fracture surface from 4.0 inch to 13.0 inch, from 20.0 inch to 23.0 inch, and from 24.5 inch to 28.0 inch were variously tinted orange/red, blue, or purple (see Figure 15), consistent with exposure to elevated temperature. At approximately 8 inch, inside the region from 4.0 inch to 13.0 inch, the P3 seam appeared to be fractured completely through the seam over a distance of approximately 1 inch and a black substance, consistent with charred asphalt was observed on the fracture surface, as shown in Figure 17. The appearance of the fracture surface at that location was consistent with quasi-cleavage fracture, segmented by thin bands of ductile fracture, consistent with fracture as a result of the rupture. No other regions were observed along the P3 seam where the seam had cracked through the wall.

Features consistent with ductile fracture originating from the root of the weld were observed, relative to the upstream end of P3 (i.e., girth weld C3), from 10.3 inch to 11.3 inch (Figure 18), from 19.5 inch to 23.1 inch (Figure 15), from 23.1 inch to 24.0 inch (Figure 19), from 31.7 inch to 33.9 inch (Figure 20), and from 40.3 inch to 40.7 inch (Figure 21). The extent of ductile fracture is indicated by a yellow-dashed line in each figure.

The ductile fracture region originating from the root of the weld in Figure 15 was examined by SEM after treatment with acetate tape. Features observed fell into one of three categories: 1) well-adhered corrosion product; 2) dimple features consistent with ductile fracture; or 3) square etch pits and step/terrace features consistent with corrosion. An example of the last is shown in Figure 22. Moving from the ductile fracture region towards the outer diameter surface, the fracture morphology changed to a specular appearance, consistent with quasi-cleavage fracture, and a blue/purple tint as previously described. The remaining silver-colored region was a result of the lab fracture and had a mixed appearance, with some regions containing features consistent with ductile fracture and other regions containing features consistent with quasi-cleavage fracture.

The region from 31.7 inch to 33.9 inch was examined at higher optical magnification and by SEM. Figure 23 shows a higher magnification image of the region labeled D in Figure 20. Alternating light-colored and dark-colored bands were observed aligned approximately with the longitudinal direction. The bands were of a comparatively close spacing near the weld root and of an increased spacing moving away from the weld root.

Examination by SEM indicated that the alternating light/dark bands were due to a change in the morphology of the fracture surface. Figure 24a shows an SEM micrograph of the region labeled E in Figure 23. A higher magnification micrograph is shown in Figure 24b (box b in Figure 24a). The fracture surface had an appearance consistent with a smeared fracture surface, with occasional observable dimple features. Figure 23c (box c in Figure 24a) shows the morphology of the dark-colored region, where ductile dimples had not been deformed. Similar light/dark banding was observed from 40.3 inch to 40.7 inch, as shown in Figure 21.

The wall thickness, weld depth, and unwelded depth along the P2 and P3 longitudinal seams were measured using a micrometer and calibrated digital images. A shear lip had formed along parts of the P2 and P3 outer diameter surface making optical measurements of the wall thickness unreliable, so a micrometer was used to measure the wall thickness, taking care to avoid the shear lip region. The unwelded depth was measured on calibrated optical images and the welded depth was calculated as the difference between the two. Ten measurements, spaced 4 inch apart, were made along each seam. The average values for wall thickness, weld depth, and unwelded depth are given in Table 1. P1 wall thickness and weld depth data are provided for comparison (NTSB, 2011a). Average values are given with and without the first and last measurement along the seam, as in some instances, those values deviated from the average by more than two standard deviations and their location was not random but correlated with the ends of the pipe. Note that the measurements for P1 were taken on the CCW side of the seam. There was a 0.030 inch high/low offset across the P1 seam. Wall thickness and unwelded depth measurements are greater on the CW side of the seam by approximately 0.030 inch. The individual weld and wall thickness measurements for P2 and P3 are given in Appendix B.

The angle on the inside of the pipe between mating sides of the pup 3 longitudinal seam was measured on a cross section macrograph of the seam (NTSB, 2011a). Because of bending deformation to the seam, the angle was measured using two approaches:

1) By assuming that, prior to the rupture, the outside surface of the pipe was originally flat across the bend where the external weld reinforcement had been removed by grinding;
2) By assuming that, prior to the rupture, the mating edges of the seam were originally parallel.

The measured angle on the inside of the pipe was 7° and 10° for the first and second approach, respectively.

The circumference of each length of pipe was measured using a steel tape. The data are shown in Table 2. LS was measured twice. The first measurement was in the southern section where there was no longitudinal fracture. The second measurement was just upstream of P1 where LS was fractured in the longitudinal direction. The deformation to the pipe along the longitudinal fracture (see Figure 4a and b in NTSB (2011a)) reduced the circumference by 0.25 inch. The fracture spanned all of P1 and part of P2 as well. The P2 measurement was taken 3 inch from its downstream end where the seam was partly intact. The longitudinal fracture circumference values were consistent with nominal 30-inch diameter pipe.

C.2. LONGITUDINAL SEAM WELD MICROSTRUCTURE AND MICROHARDNESS

The longitudinal seam weld microstructure of LS, P6, and LN were compared with the weld microstructure of P1, P2, and P3. Figure 25a shows the weld microstructure observed on a cross section of the LS longitudinal seam, which was typical of the microstructure observed on P6 and LN, as well. Figure 25b shows the weld microstructure observed on a cross section of P1, which was typical of P2, and P3, as well. The LS longitudinal seam weld had a much finer microstructure than the weld along the P1 longitudinal seam, consistent with a different rate of heat input and total heat input.

The mechanical properties of the longitudinal seam welds and surrounding material were evaluated by Vickers hardness testing. Centerline hardness profiles were constructed for each weld starting at the root of the weld and progressing toward the outer surface, except for P2 and P3. For double submerged arc welds (DSAW), the hardness profile was measured from the inner diameter surface to the outer diameter surface, but for comparison, the hardness profile was plotted starting at the root of the inner seam weld progressing toward the inner diameter surface.[2] The centerline profiles were measured on each seam by grinding 0.005 inch of material from each sample cross section, and polishing the surface to a 0.05 μm alumina polish, according to standard practices (ASTM, 2001). A 500 gm load and 10 s dwell time were used for the tests. The longitudinal seam welds for P1, P2, and P3 were fractured as a result of the rupture. Hardness profiles along the centerline of the welds on P2 and P3 could not be conducted (the centerline of the weld was sufficiently offset from the fracture on P1). For P2 and P3, four hardness profiles were performed perpendicular to the fracture, two on either side of the fracture, into the weld. Hardness measurements decreased with distance from the fracture until a baseline value was reached. The average hardness was calculated using values consistent with the baseline. The data are collected in Appendix C.

Hardness was also measured for each length of pipe for the coarse-grained heat-affected zone (HAZ), grain-refined HAZ, and base metal regions. A typical example is shown for LN in Figure 26. The coarse-grained HAZ was adjacent to the weld and

[2] The inner seam weld was chosen because the outer portion of the seam was welded first and, therefore, was subject to microstructural changes that reduced its hardness during the welding of the inner portion of the seam (an average of 12 HV_{500}).

gradually transitioned to the grain-refined HAZ, which in turn transitioned to the base metal region. One side of the P2 longitudinal seam did not exhibit a coarse-grained HAZ, but rather had a highly grain-refined region where a coarse-grained HAZ was observed on other welds, as shown in Figure 27. The refined grain structure was consistent with the remnants of a previous welding pass.

The microhardness profiles for each length of pipe (excluding P2 and P3) are shown in Figure 28a through h. The average hardness for each length of pipe is shown in Figure 29 and Table 3. The mean hardness for LS, P6, and LN were 192 HV_{500}, 191 HV_{500}, 191 HV_{500}, respectively. The mean hardness for P1, P2, P3, and P5 were 159 HV_{500}, 158 HV_{500}, 155 HV_{500}, and 191 HV_{500}, respectively.

The hardness profile of the inner and outer welds on P4 varied with distance from the root. The inner weld had a low-hardness region near the root of the weld and a high-hardness outer-region that is plotted separately in Figure 29. The outer weld was comprised of two passes. The first pass and second pass are plotted separately in Figure 29 as well.

The coarse-grained HAZ, grain-refined HAZ, and base metal hardness data are shown in Table 4. The yield strength and tensile strength from NTSB (2011b) were correlated with the Vickers hardness data as shown in Figure 30a and b. A fourth order polynomial regression was fit to the yield strength data:

$$\sigma_{ys} = -1306638 + 35348.5HV - 344.877HV^2 + 1.46812HV^3 - 0.00227721HV^4$$

A linear regression was fit to the tensile strength data:

$$\sigma_{UTS} = 7.0622 + 0.4075HV$$

The complete Vickers hardness data set is presented in Appendix C.

D. REFERENCES

ASTM. (2001). *ASTM Standard E3, 2001, Standard Practice for Preparation of Metallographic Specimens*. DOI: 10.1520/E0003-01, West Conshohocken, PA: ASTM International.
NTSB. (2011a). *Docket Number SA-534 — Exhibit No. 3-A — Metallurgical Group Chairman Factual Report*. Washington, DC: National Transportation Safety Board.
NTSB. (2011b.) *Docket Number SA-534 — Exhibit No. 3-B — Metallurgical Group Chairman Factual Report*. Washington, DC: National Transportation Safety Board.

Donald Kramer
Materials Engineer

Table 1: Average wall thickness, weld depth, and unwelded depth measurements for P1, P2, and P3. Averages are given with and without the first and last measurement along the longitudinal seam, as in some instances, the first and last measurements deviated from the mean by more than two standard deviations and their location was not random but correlated with the ends of the pipe. The measurements for P1 were taken on the counterclockwise side of the seam. There was a 0.030 inch high/low offset across the P1 seam. Wall thickness and unwelded depth measurements are greater on the clockwise side of the seam by 0.030 inch. See the metallurgical cross section of the P1 longitudinal seam in NTSB (2011a). Confidence intervals are given as one standard deviation.

First and Last Measurement Included			
Pipe Length	**Wall Thickness, inch**	**Weld Depth, inch**	**Unwelded Depth, inch**
P1	0.312 ± 0.015	0.172 ± 0.025	0.140 ± 0.021
P2	0.368 ± 0.005	0.201 ± 0.035	0.168 ± 0.031
P3	0.353 ± 0.006	0.160 ± 0.013	0.192 ± 0.016
First and Last Measurement Excluded			
Pipe Length	**Wall Thickness, inch**	**Weld Depth, inch**	**Unwelded Depth, inch**
P1	0.309 ± 0.015	0.162 ± 0.017	0.147 ± 0.018
P2	0.369 ± 0.006	0.195 ± 0.036	0.174 ± 0.031
P3	0.352 ± 0.006	0.162 ± 0.014	0.190 ± 0.017

Table 2: Pipe circumference measured by steel tape. LS was measured twice; 1) upstream of where the longitudinal fracture terminated and 2) just upstream of P1 along the longitudinal fracture. The fracture spanned all of P1 and part of P2 as well. The P2 measurement was taken 3 inch from its downstream end where the seam was partly intact.

Pipe Length	Circumference, inch
LS – No Fracture	94.25
LS – Longitudinal Fracture	94.00
P1	94.25
P2	94.56
P3	94.56
P4	94.38
P5	94.25
P6	94.38
LN	94.44

Table 3: Mean Vickers hardness of the final weld pass for all lengths of pipe. For LS, P6, and LN, the inner pass was the final pass. The inner and outer passes were combined for P5.

Pipe Length	**Hardness of Final Pass, HV_{500}**
LS	192 ± 4
P1	159 ± 5
P2	158 ± 8
P3	155 ± 6
P4[3]	177 ± 15
P5	191 ± 3
P6	191 ± 5
LN	191 ± 6

Table 4: Hardness values in the coarse-grained heat-affected zone (HAZ), grain-refined HAZ, and base metal. Confidence intervals are given as one standard deviation.

Pipe Length	**Coarse-Grained HAZ Hardness, HV_{500}**	**Grain-Refined HAZ Hardness, HV_{500}**	**Base Metal Hardness, HV_{500}**
LS	208 ± 11	185 ± 4	183 ± 9
P1	198 ± 16	147 ± 5	141 ± 6
P2	152 ± 10	114 ± 5	115 ± 5
P3	171 ± 19	136 ± 5	127 ± 5
P4	201 ± 9	185 ± 8	172 ± 7
P5	231 ± 12	191 ± 6	153 ± 9
P6	201 ± 8	175 ± 6	176 ± 8
LN	209 ± 10	188 ± 8	182 ± 8

[3] The hardness for the final weld pass on P4 was not constant but varied continuously from 160 HV_{500} at the root to 200 HV_{500} at the outer surface.

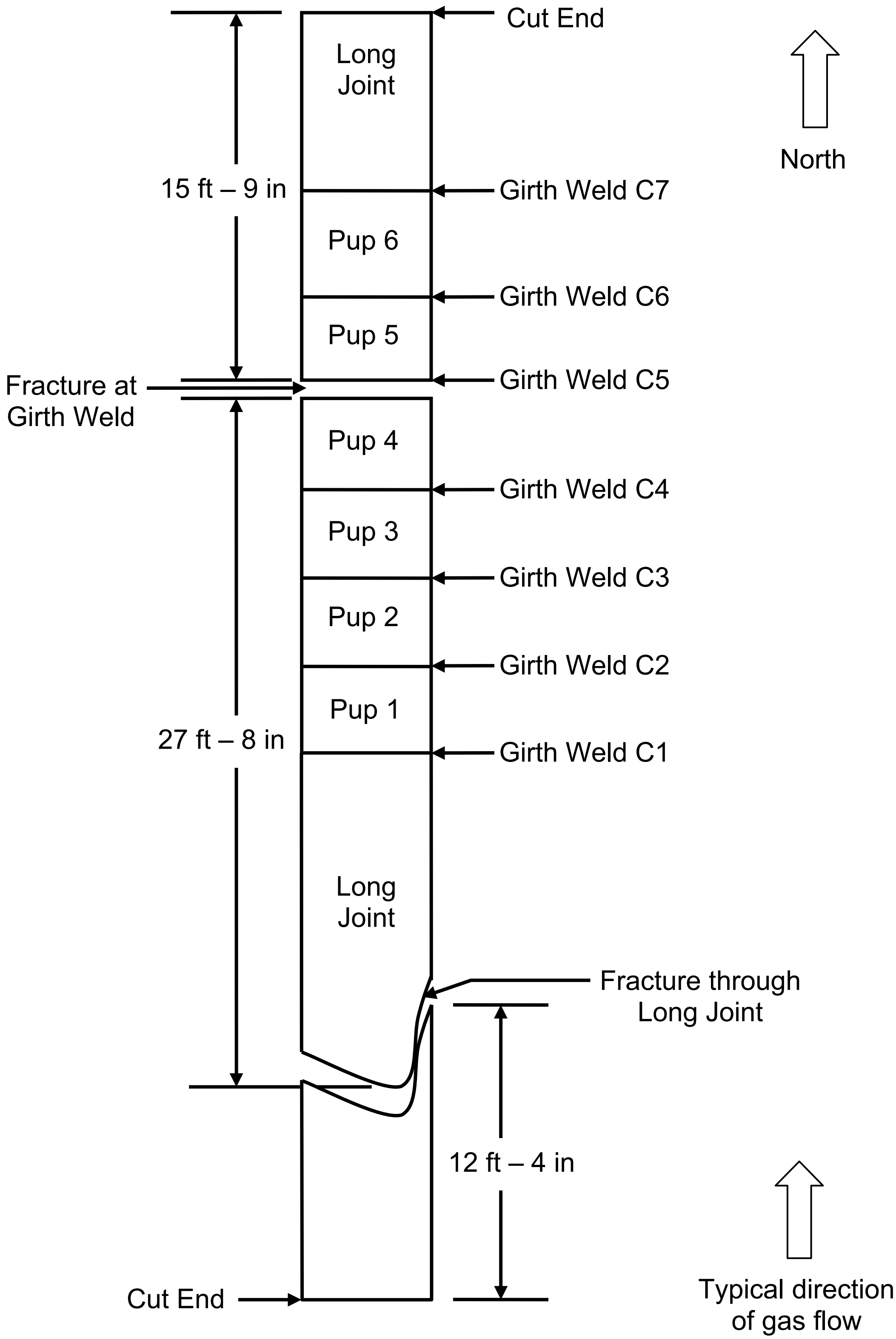

Figure 1: Schematic of pipe showing location of girth welds and fractures. Longitudinal fracture not depicted.

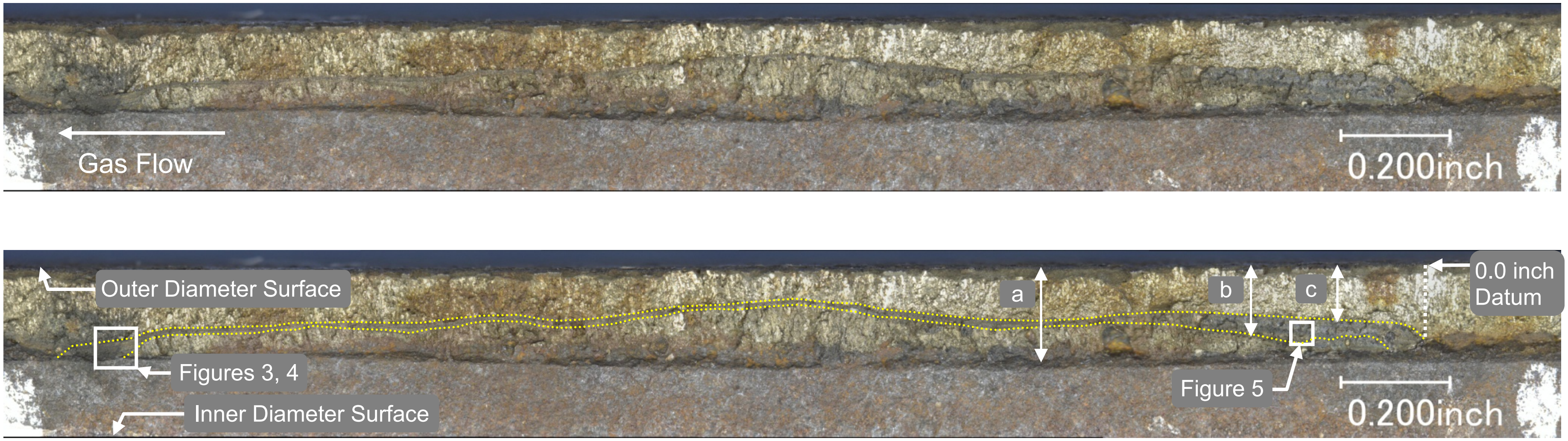

Figure 2: Clockwise fracture face of the initiation site located in P1. The lower yellow line follows the crack boundary after progression by overstress. The upper yellow line follows the crack boundary after progression by overstress and fatigue. Features consistent with fatigue fracture were located between the two dashed yellow lines. Intact wall thickness measurements were made approximately every 0.10 inch for; a) the weld depth; b) intact wall thickness after progression of the crack by overstress; and c) intact wall thickness after progression of the crack by overstress and fatigue.

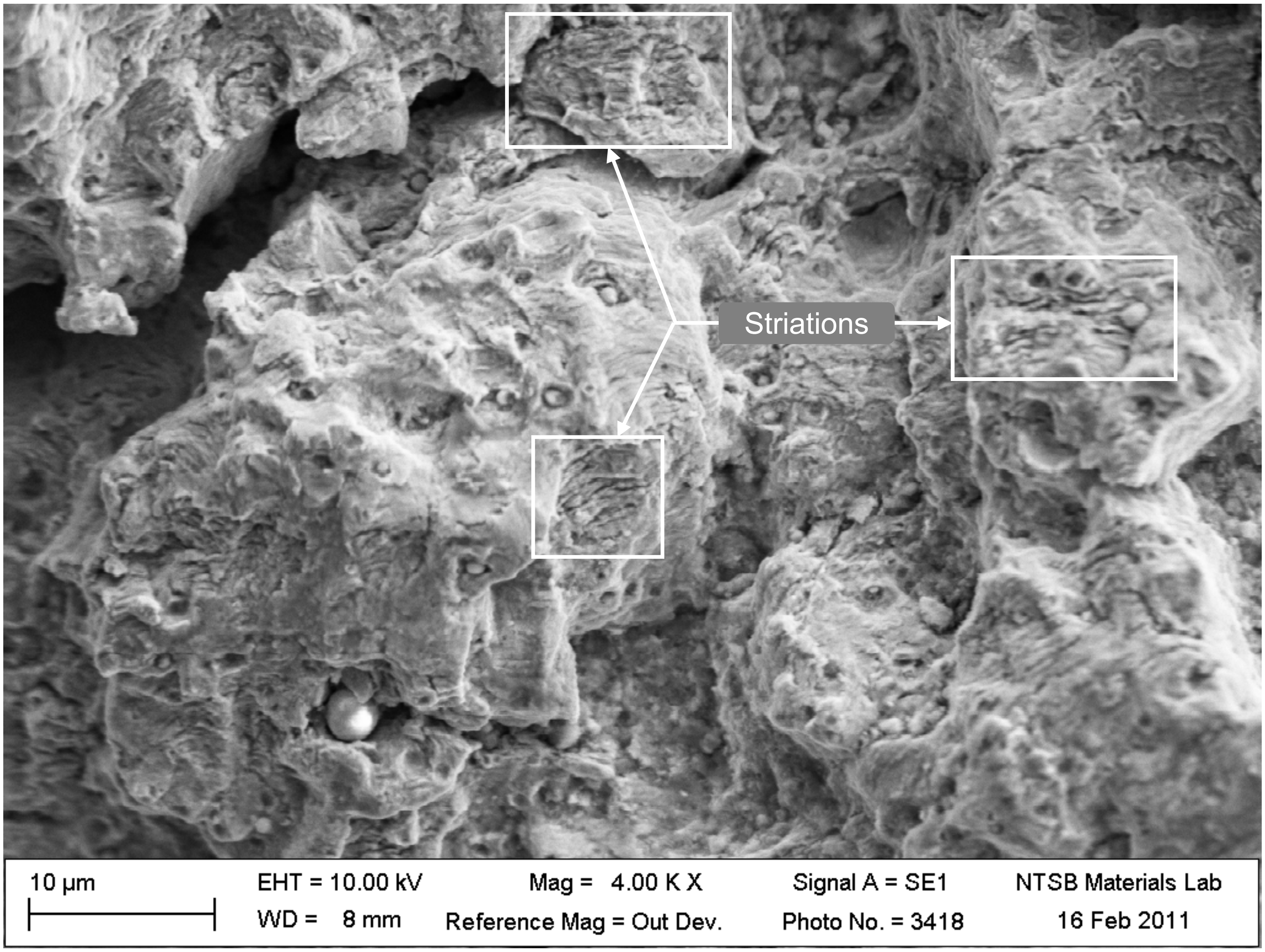

Figure 3: SEM micrograph of the P1 CW longitudinal seam weld fracture within the area bordered by the two yellow-dashed lines in Figure 2. Striated features were observed on the fracture surface, consistent with fatigue.

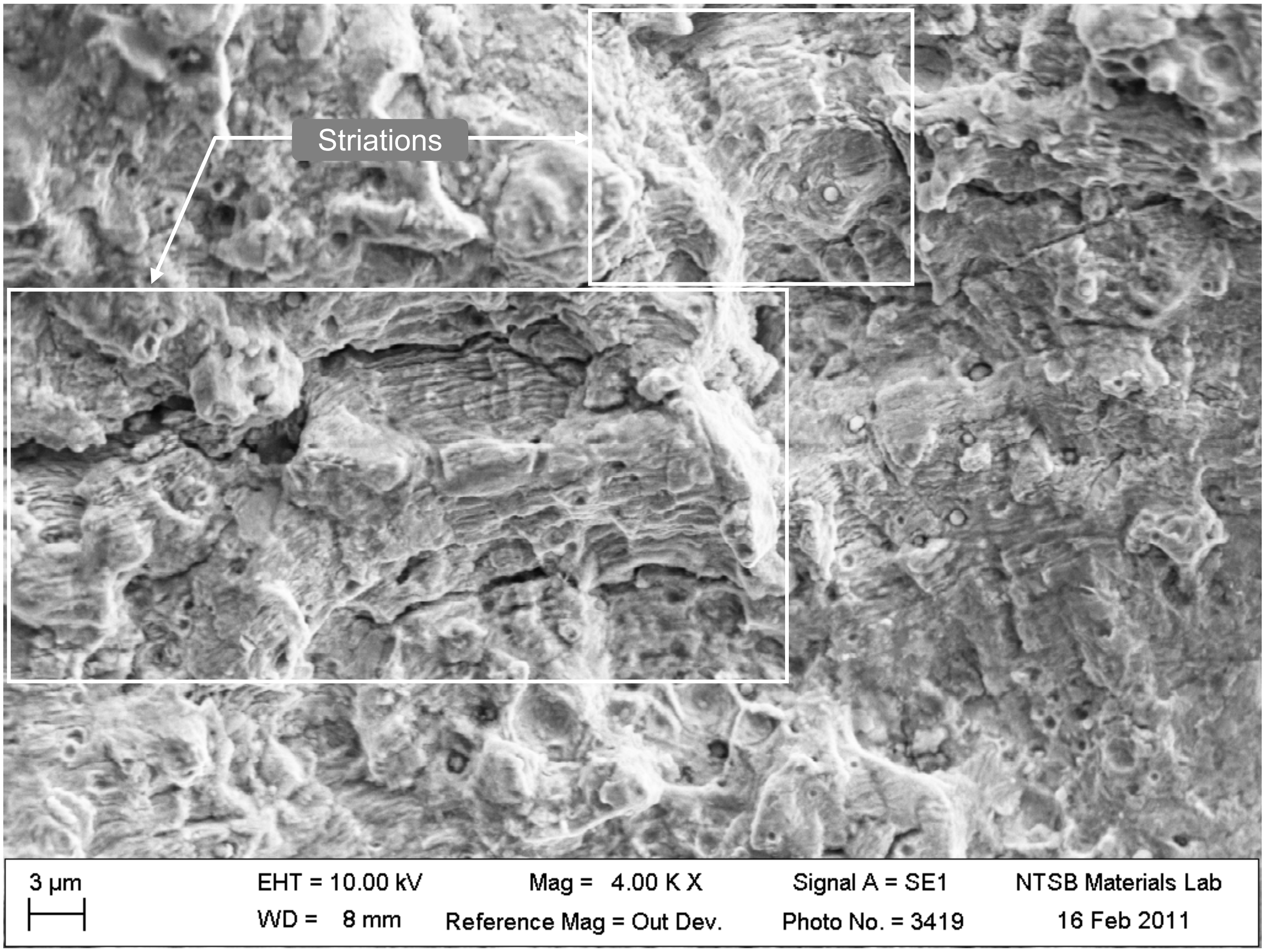

Figure 4: SEM micrograph of the P1 CW longitudinal seam weld fracture within the area bordered by the two yellow-dashed lines in Figure 2. Striated features were observed on the fracture surface, consistent with fatigue.

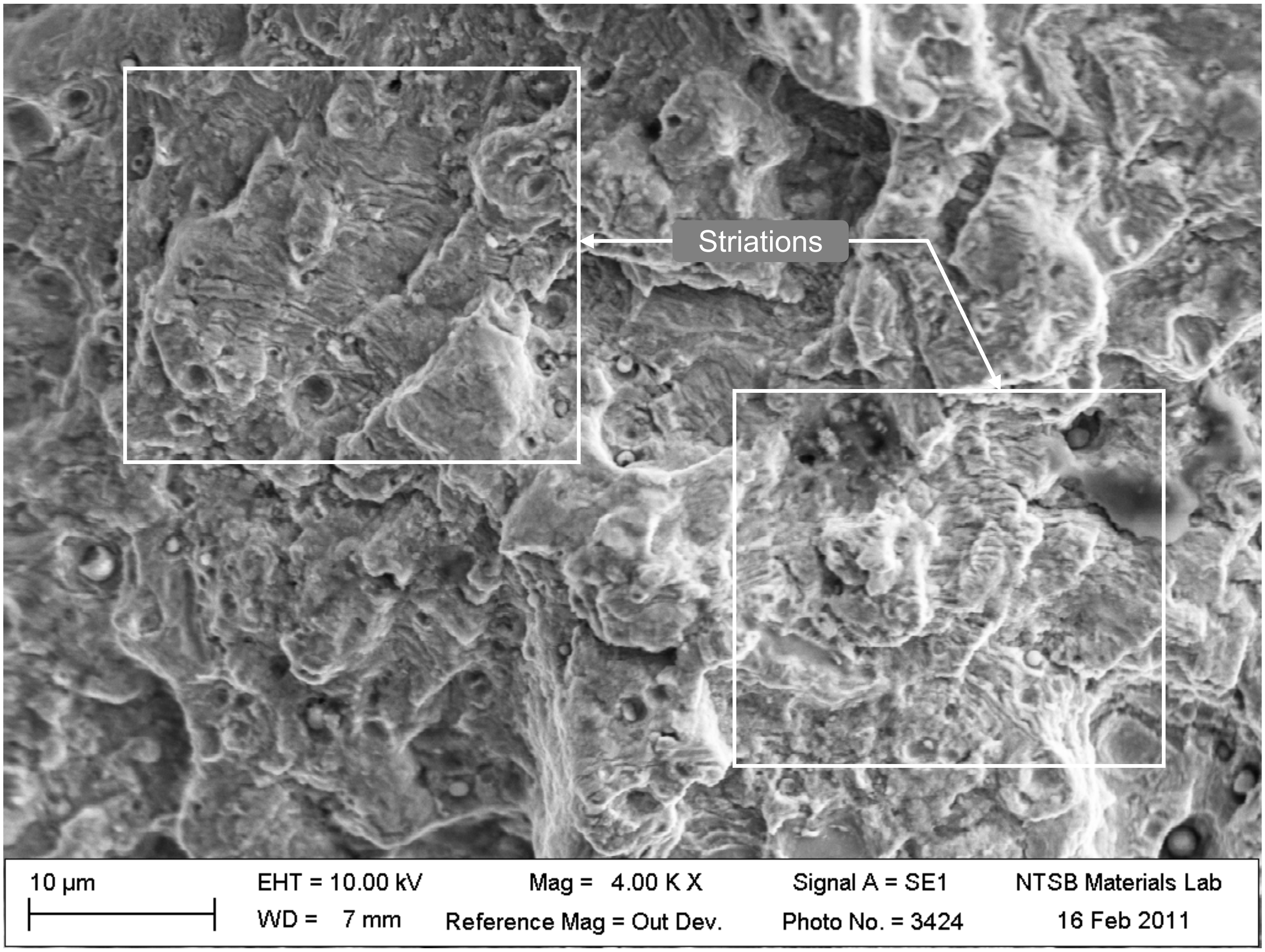

Figure 5: SEM micrograph of the P1 CW longitudinal seam weld fracture within the area bordered by the two yellow-dashed lines in Figure 2. Striated features were observed on the fracture surface, consistent with fatigue.

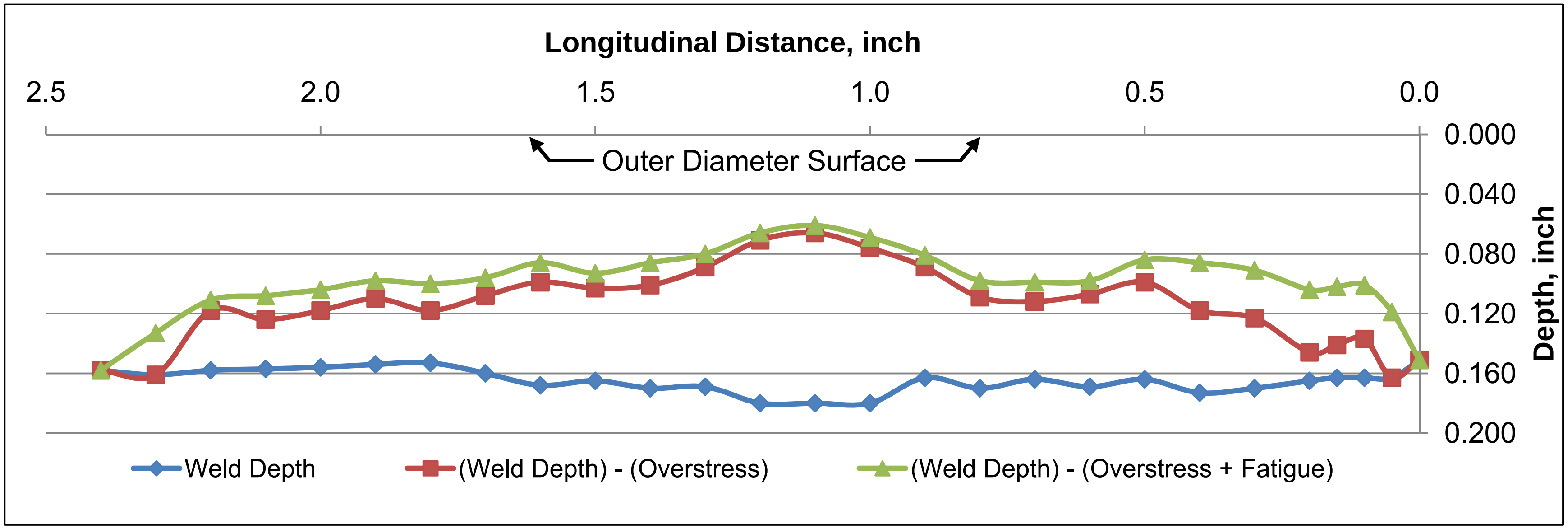

Figure 6: Depth measurements at the crack initiation site along the P1 CW longitudinal seam. Depth measurements are referenced with respect to the outer surface of the pipe; weld depth (blue diamonds), intact wall thickness after crack progression by ductile overstress (red squares), and intact wall thickness after crack progression by overstress and fatigue (green triangles).

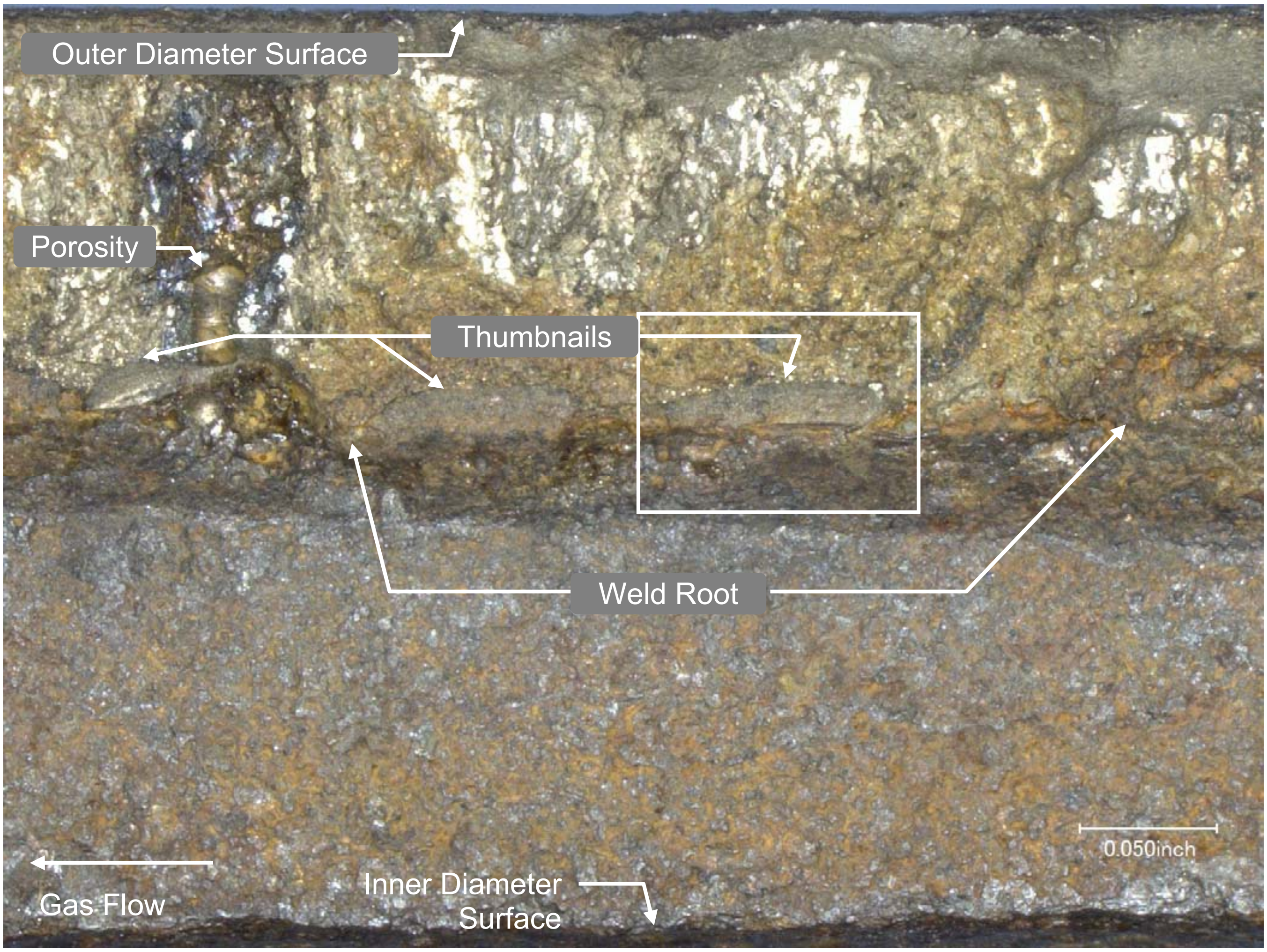

Figure 7: Optical macrograph of the P1 longitudinal seam, CW side of the seam, just upstream of the initiation site where thumbnail features were observed along the root of the weld.

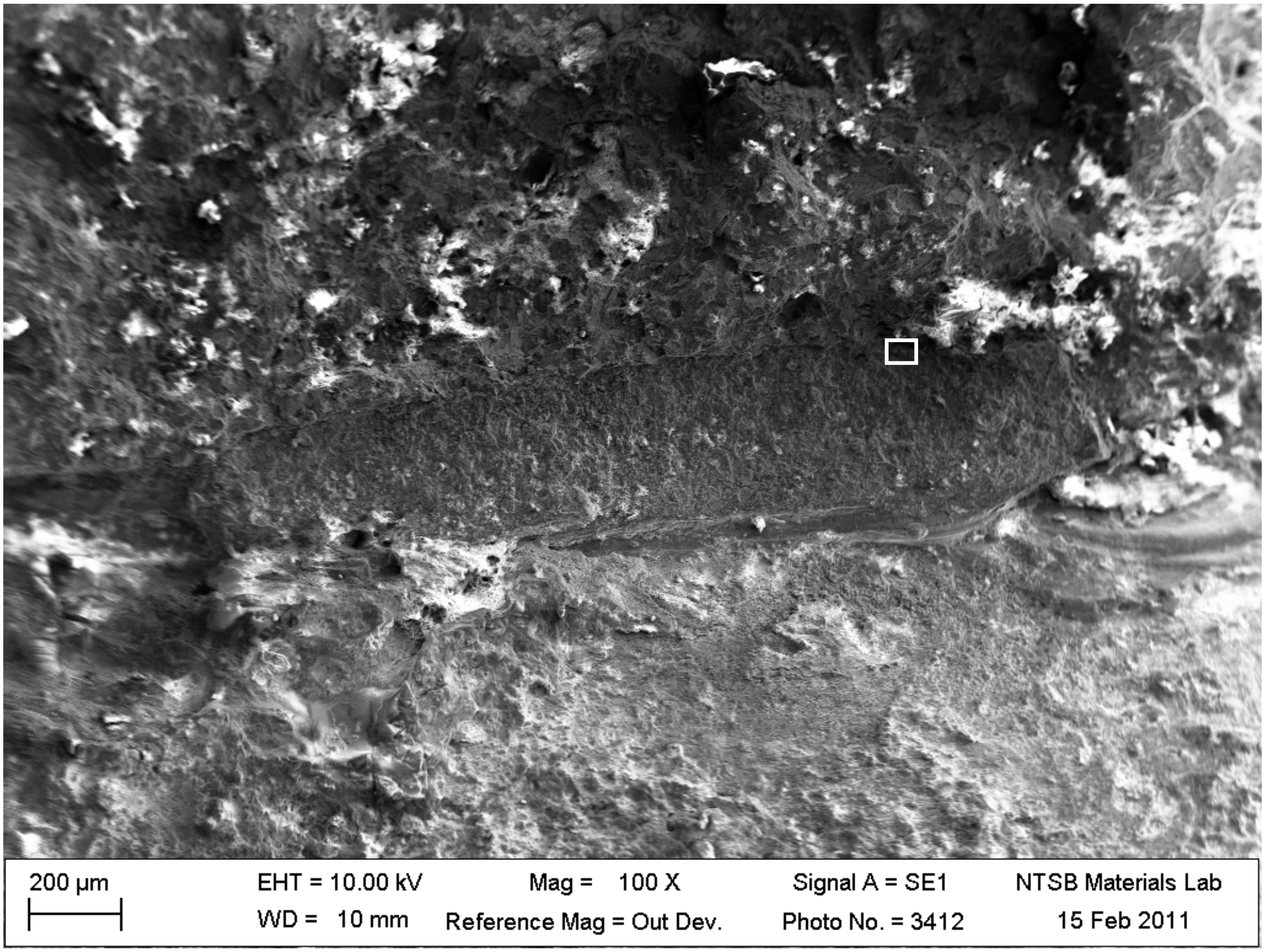

Figure 8: SEM micrograph of the thumbnail feature indicated by the box in Figure 7.

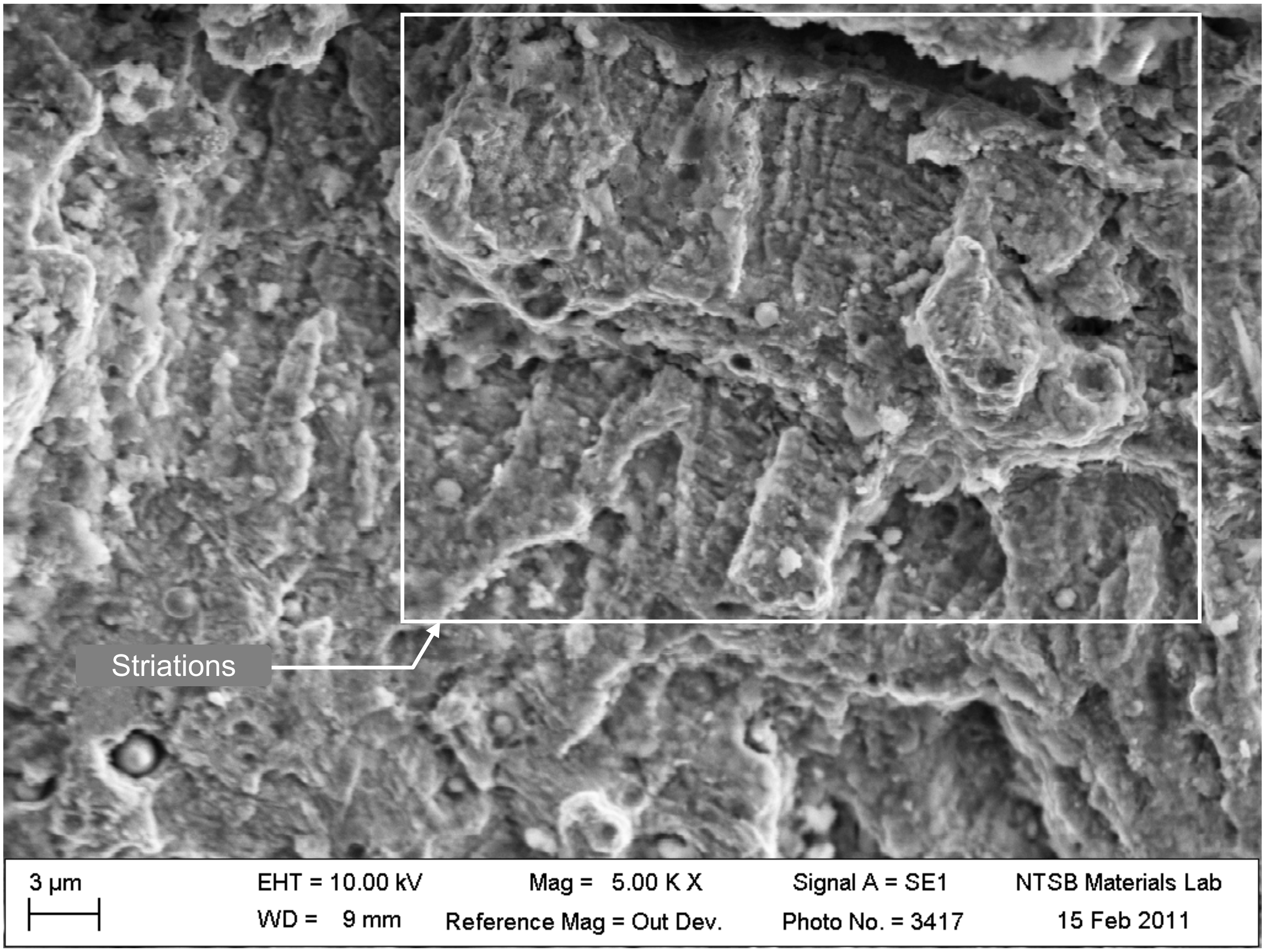

Figure 9: SEM micrograph of the P1 CW fracture face in a thumbnail feature at the root of the weld. Striations are indicated by a rectangle in the figure. The location of the micrograph is indicated by the box in Figure 8.

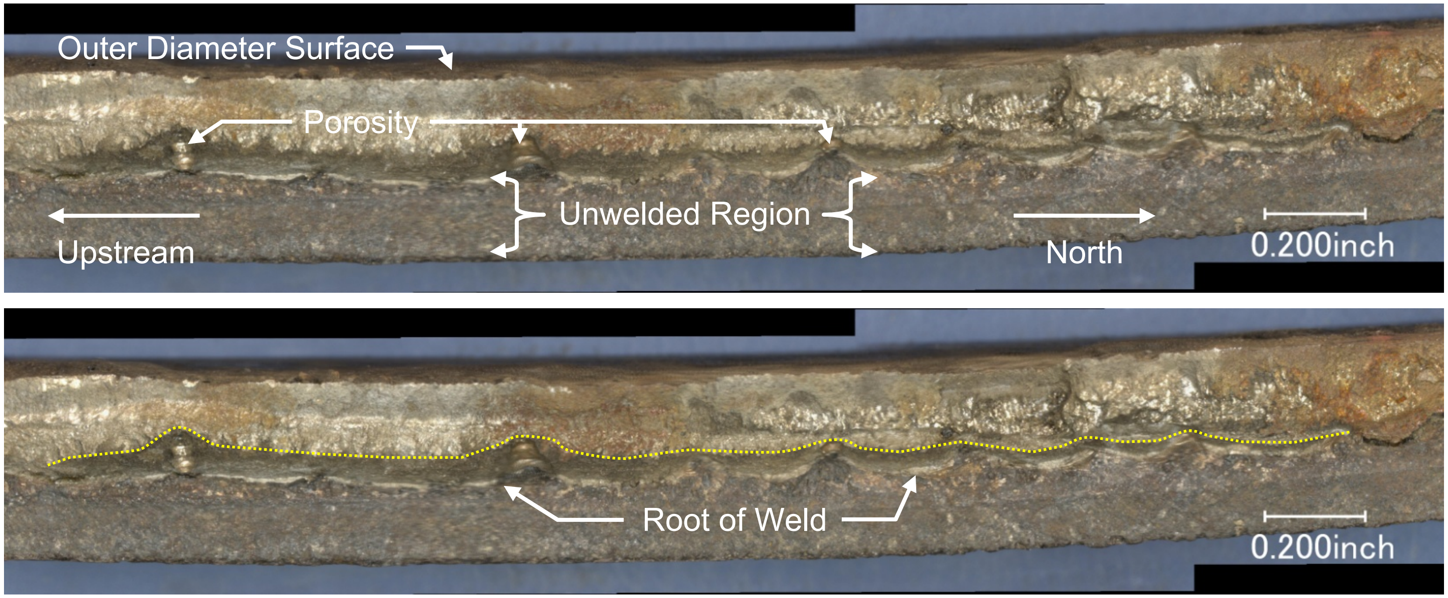

Figure 10: Region of ductile fracture originating from the root of the weld along the P2 CCW longitudinal seam. The region extended from 29.4 inch to 32.2 inch, with respect to the upstream end of P2 (girth weld C2). The dark-colored ductile fracture boundary is indicated by the yellow-dashed line in the bottom image.

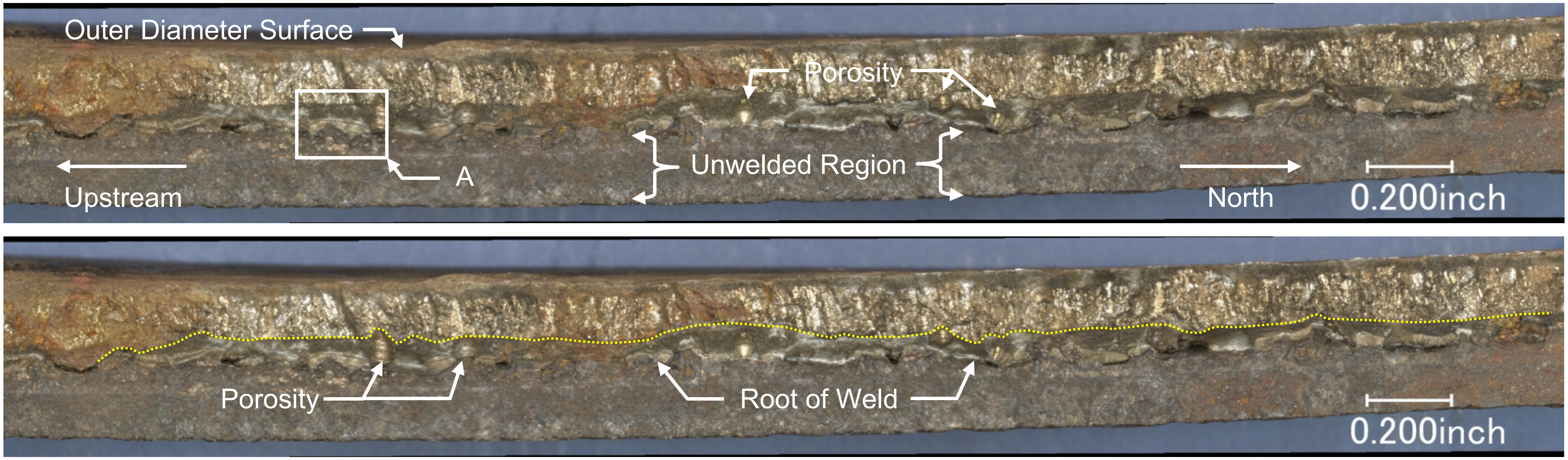

Figure 11: Region of ductile fracture originating from the root of the weld along the P2 CCW longitudinal seam. The region extended from 32.3 inch to 35.9 inch, with respect to the upstream end of P2. The ductile fracture boundary is indicated by the yellow-dashed line in the bottom image. An SEM image of region A is shown in Figure 13.

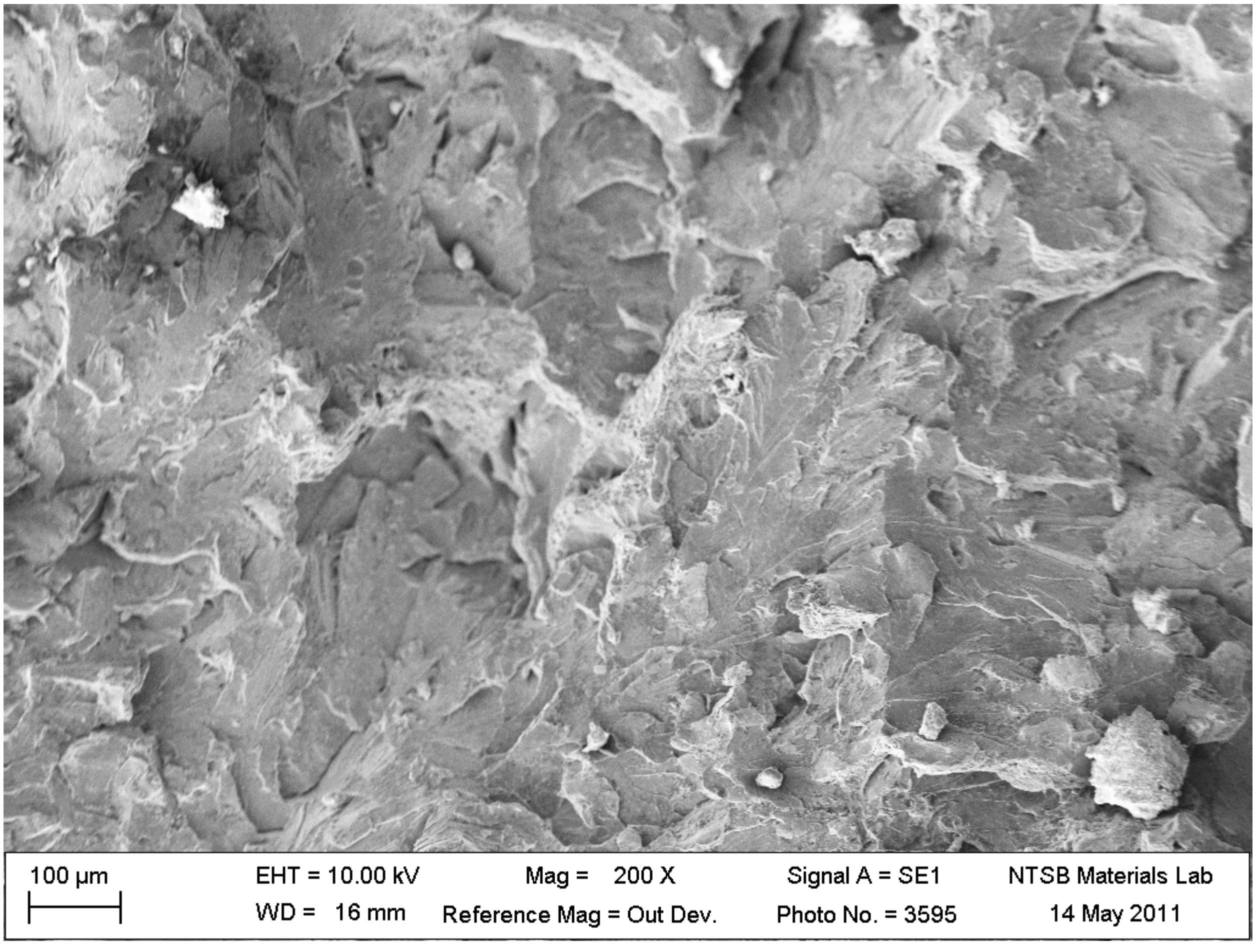

Figure 12: SEM micrograph of quasi-cleavage fracture approximately 34 inch from the upstream end of P2 along the CCW longitudinal seam.

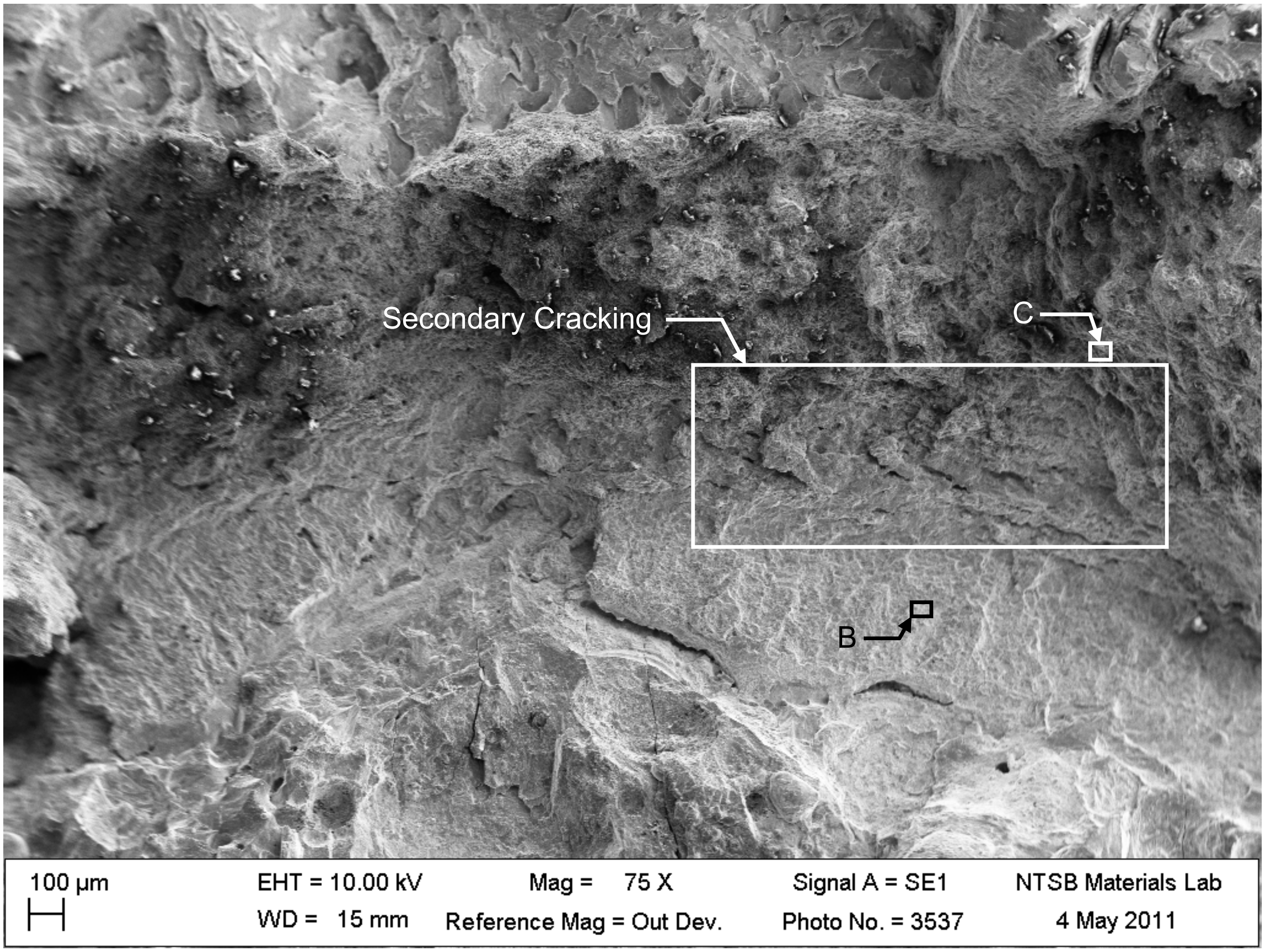

Figure 13: SEM micrograph of a ductile fracture region along the P2 CCW longitudinal seam at the area labeled A in Figure 11. Higher magnification micrographs of regions B and C are shown in Figure 14.

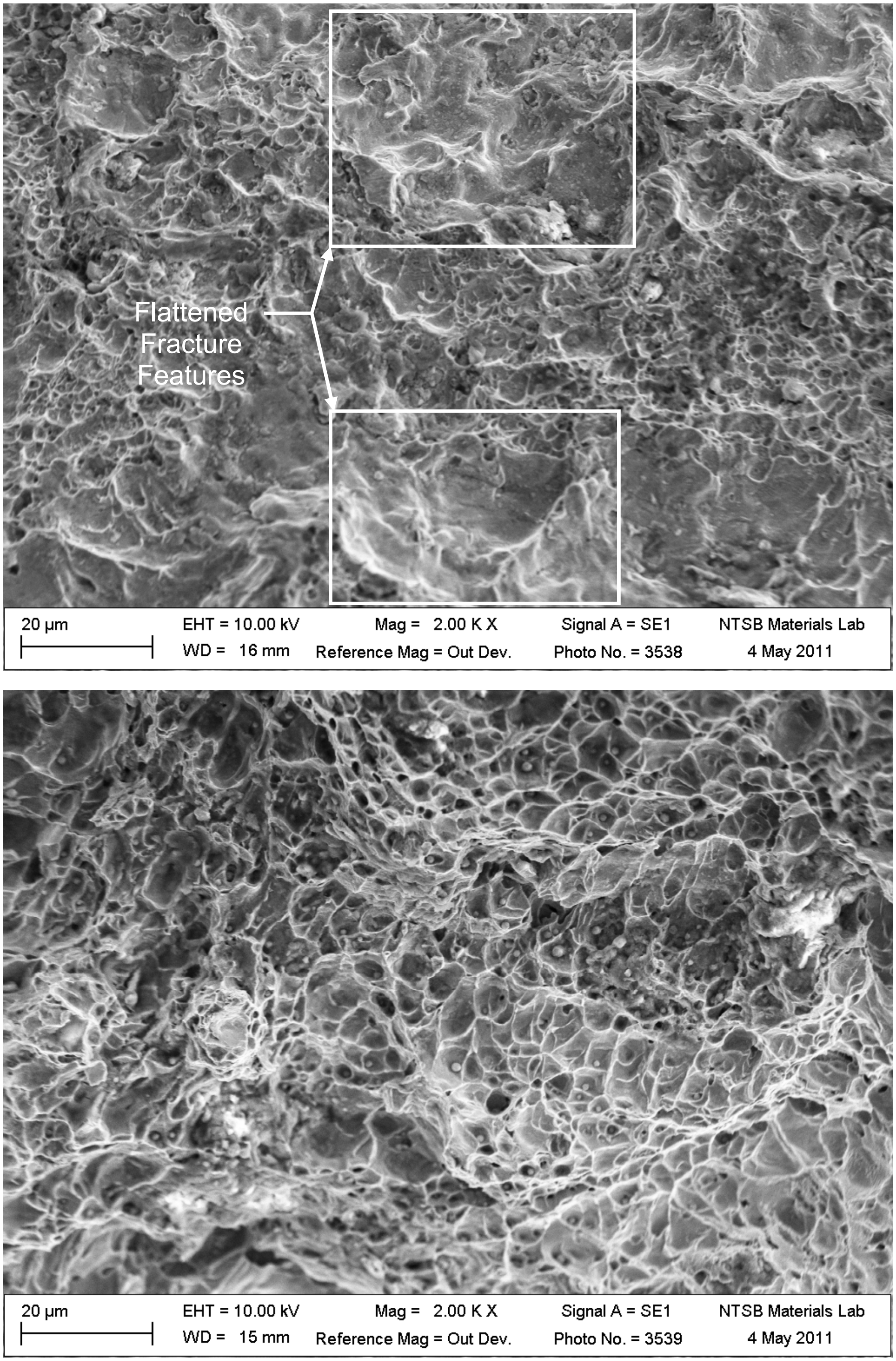

a)

b)

Figure 14: Higher magnification SEM micrographs from the regions indicated in Figure 13 along the P2 CCW longitudinal seam; a) Region B showing flattening of dimple features; b) Region C showing dimple features but little to no flattening.

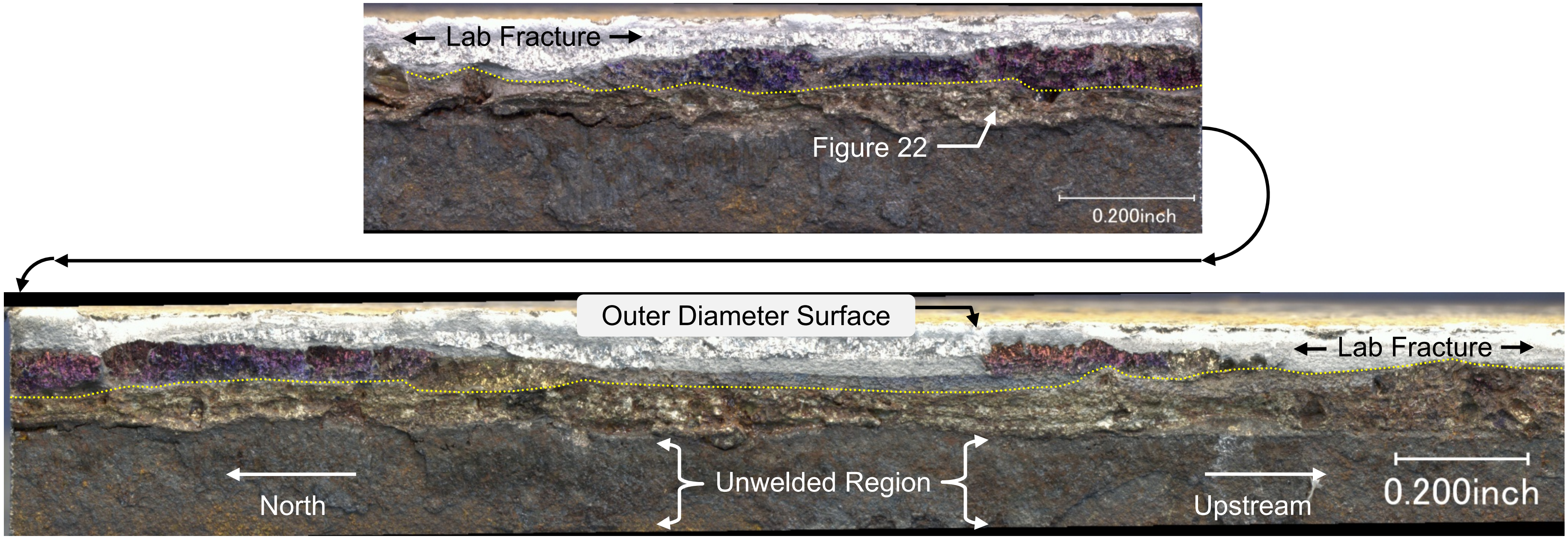

Figure 15: P3 CW longitudinal seam where features consistent with ductile fracture and corrosion were observed extending from 19.5 inch to 23.1 inch from the upstream end of P3. The right side of the top image continues on the left side of the bottom image, where a bandsaw cut was made. The lab-fractured regions had a silver color, typical of a fresh fracture.

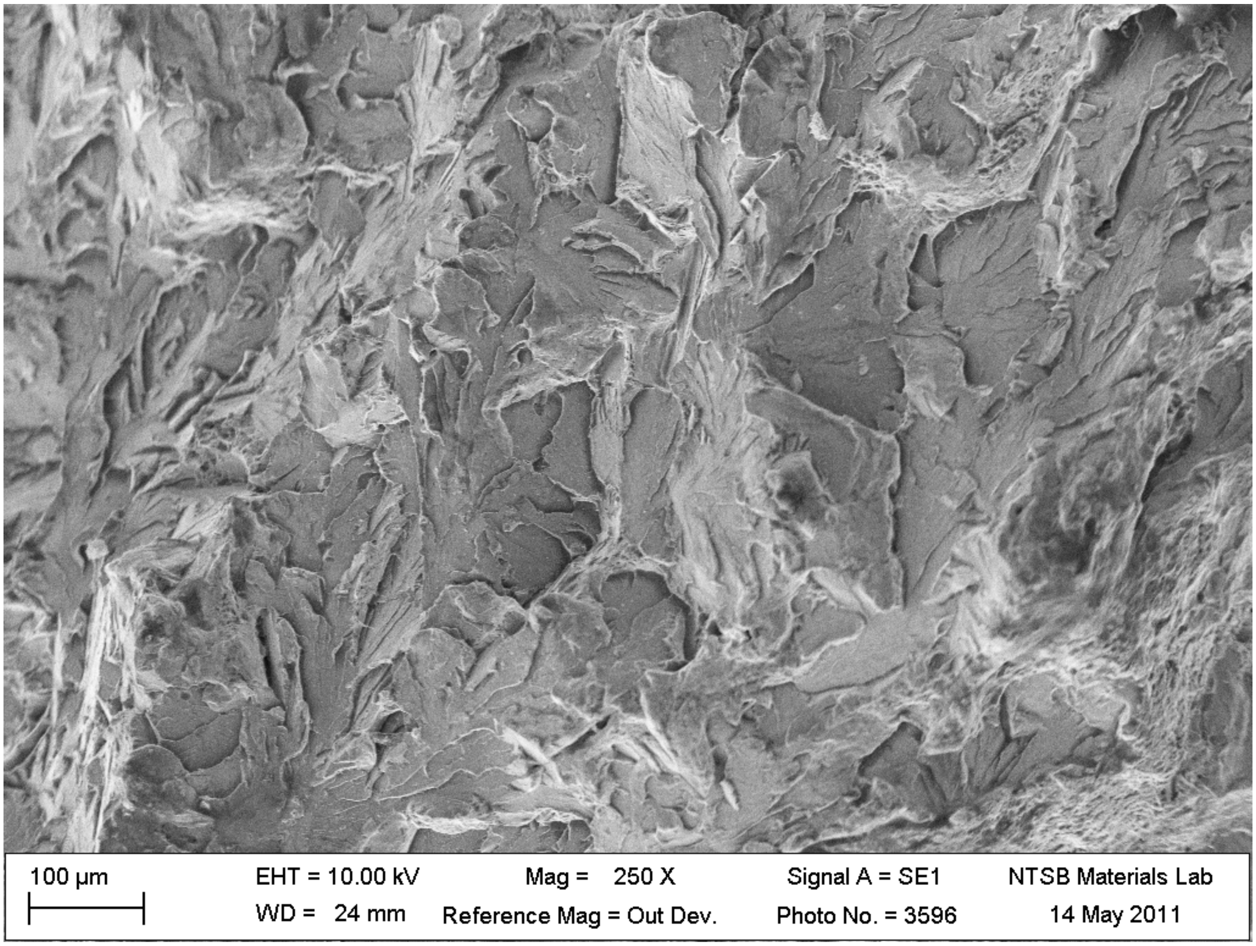

Figure 16: SEM micrograph of quasi-cleavage fracture approximately 31 inch from the upstream end of P3 along the CW longitudinal seam.

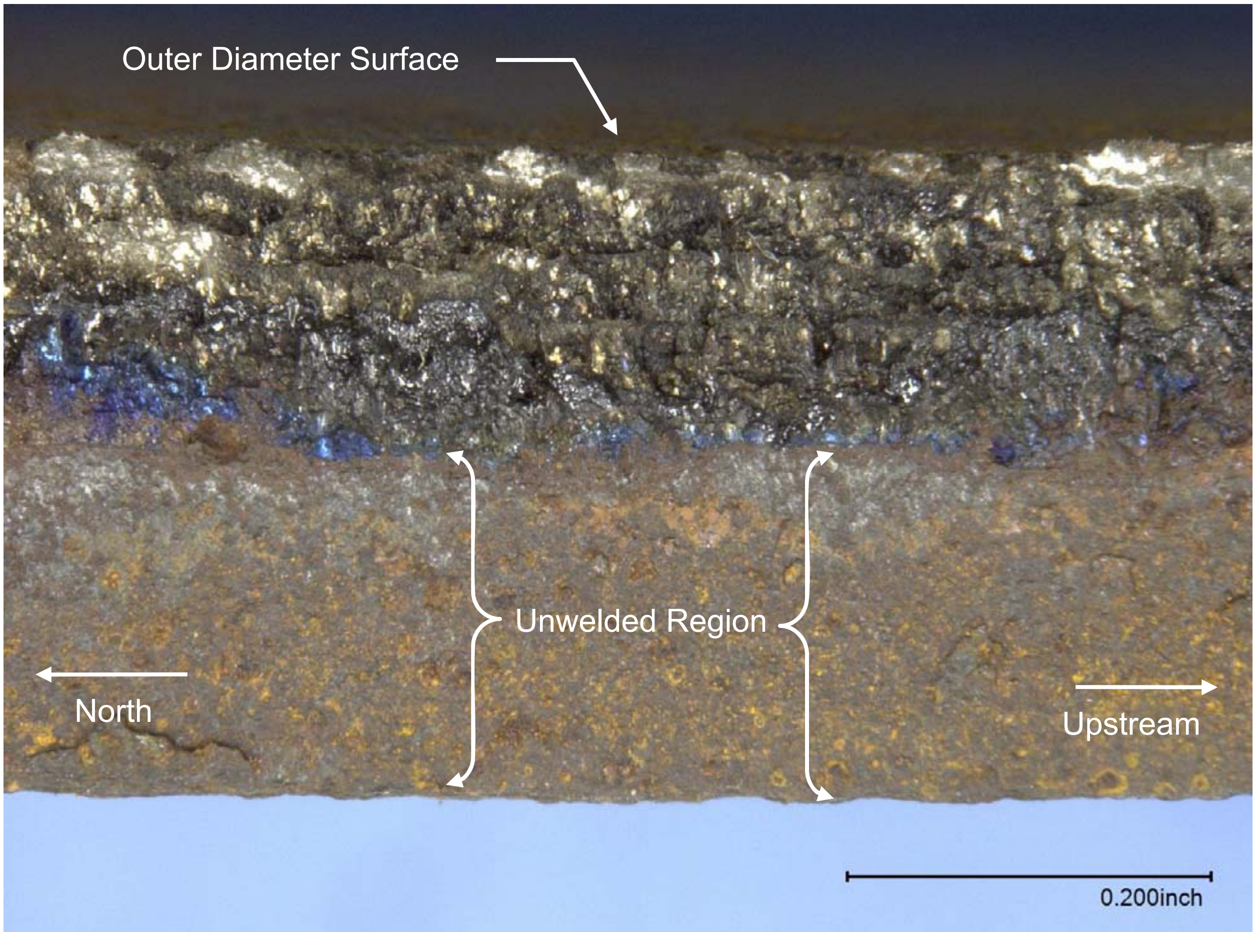

Figure 17: Photograph of the P3 CW fracture surface at approximately 8 inch from the upstream end. The fracture surface was covered by a black substance, consistent with charred asphalt. The appearance of the fracture surface was consistent with quasi-cleavage fracture, segmented by thin bands of ductile fracture.

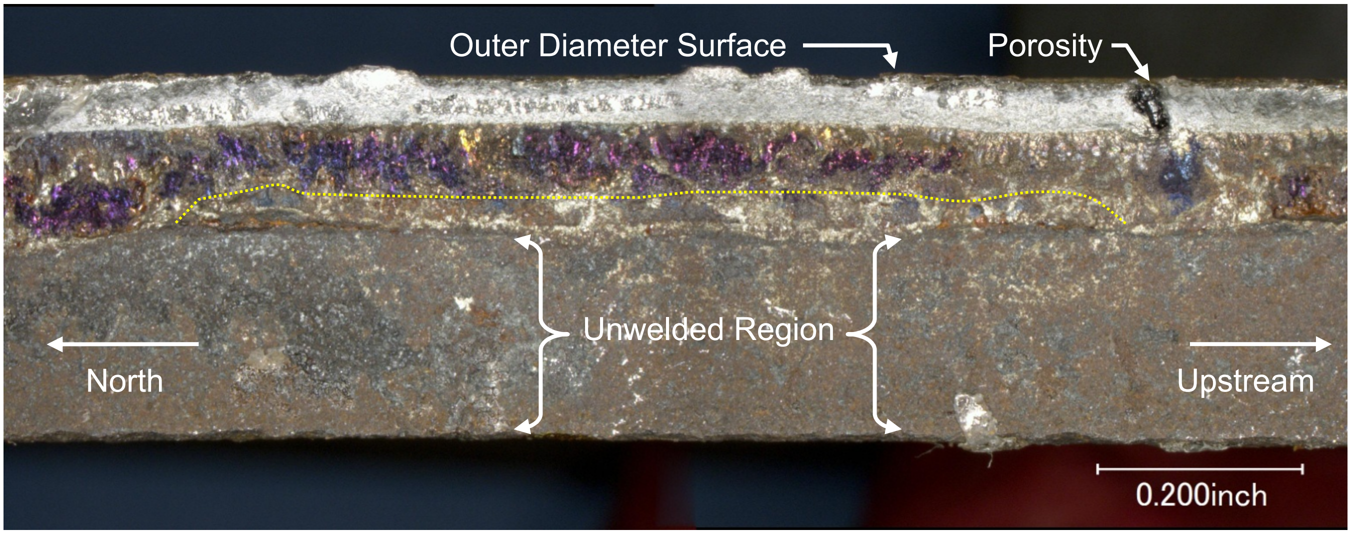

Figure 18: P3 CW longitudinal seam where features consistent with ductile fracture were observed extending from 10.3 inch to 11.3 inch from the upstream end of P3.

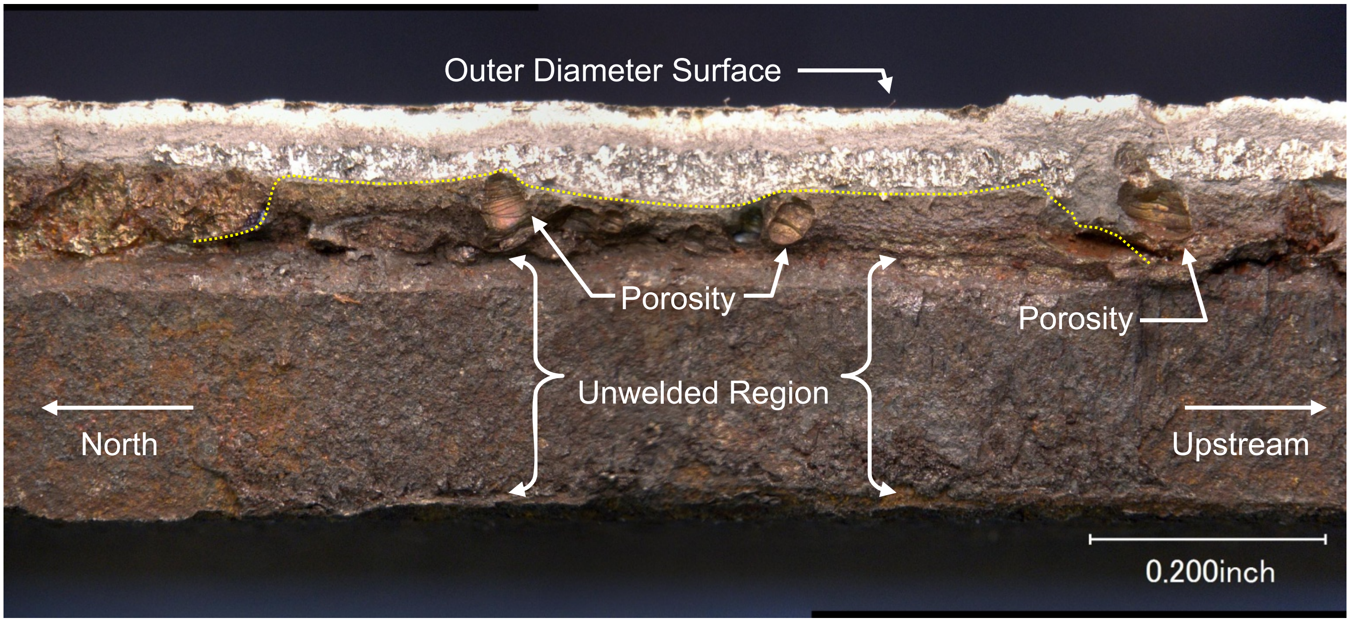

Figure 19: P3 CW longitudinal seam where features consistent with ductile fracture were observed extending from 23.1 inch to 24.0 inch from the upstream end of P3.

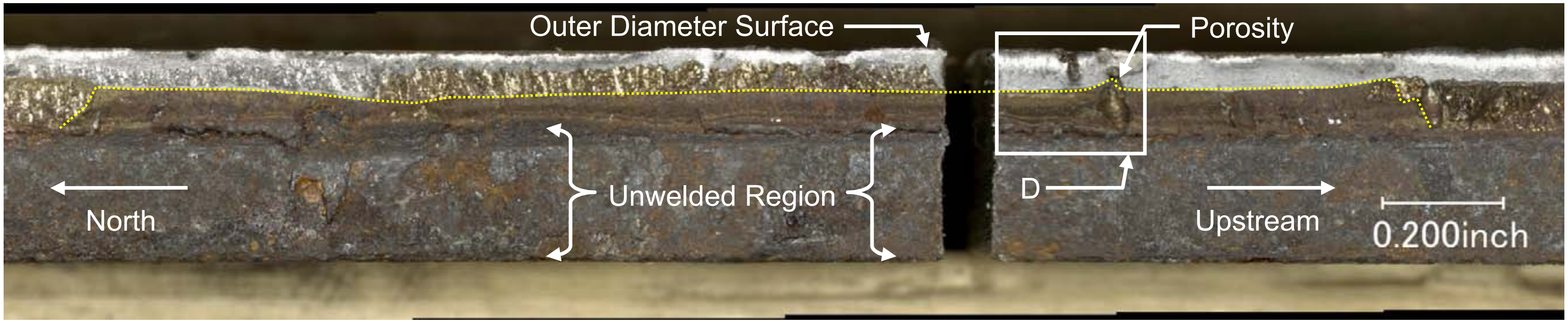

Figure 20: P3 CW longitudinal seam where features consistent with ductile fracture were observed extending from 31.7 inch to 33.9 inch from the upstream end of P3. A higher magnification optical image of the region labeled D is shown in Figure 23.

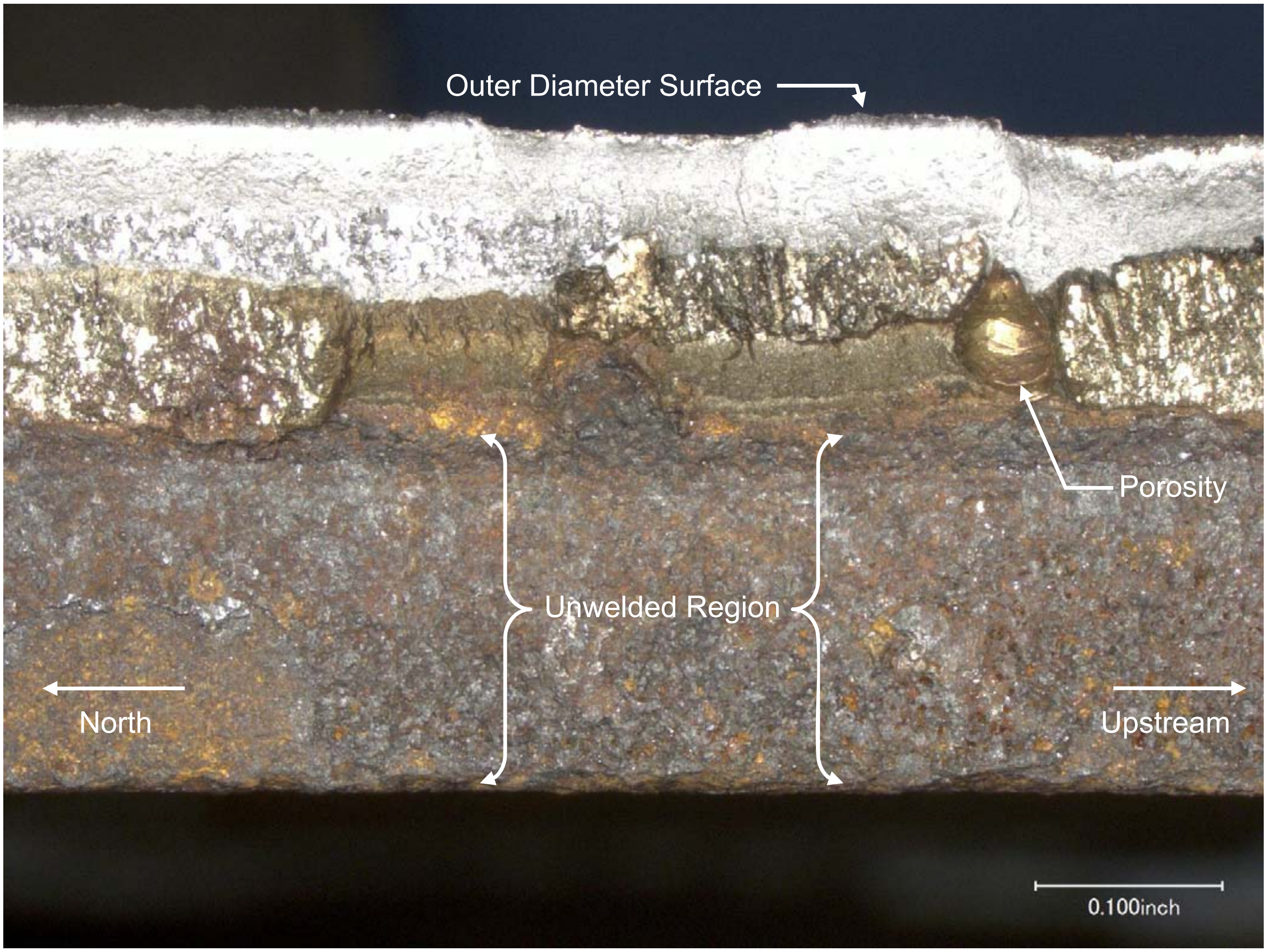

Figure 21: P3 CW longitudinal seam where features consistent with ductile fracture were observed extending from 40.3 inch to 40.7 inch from the upstream end of P3.

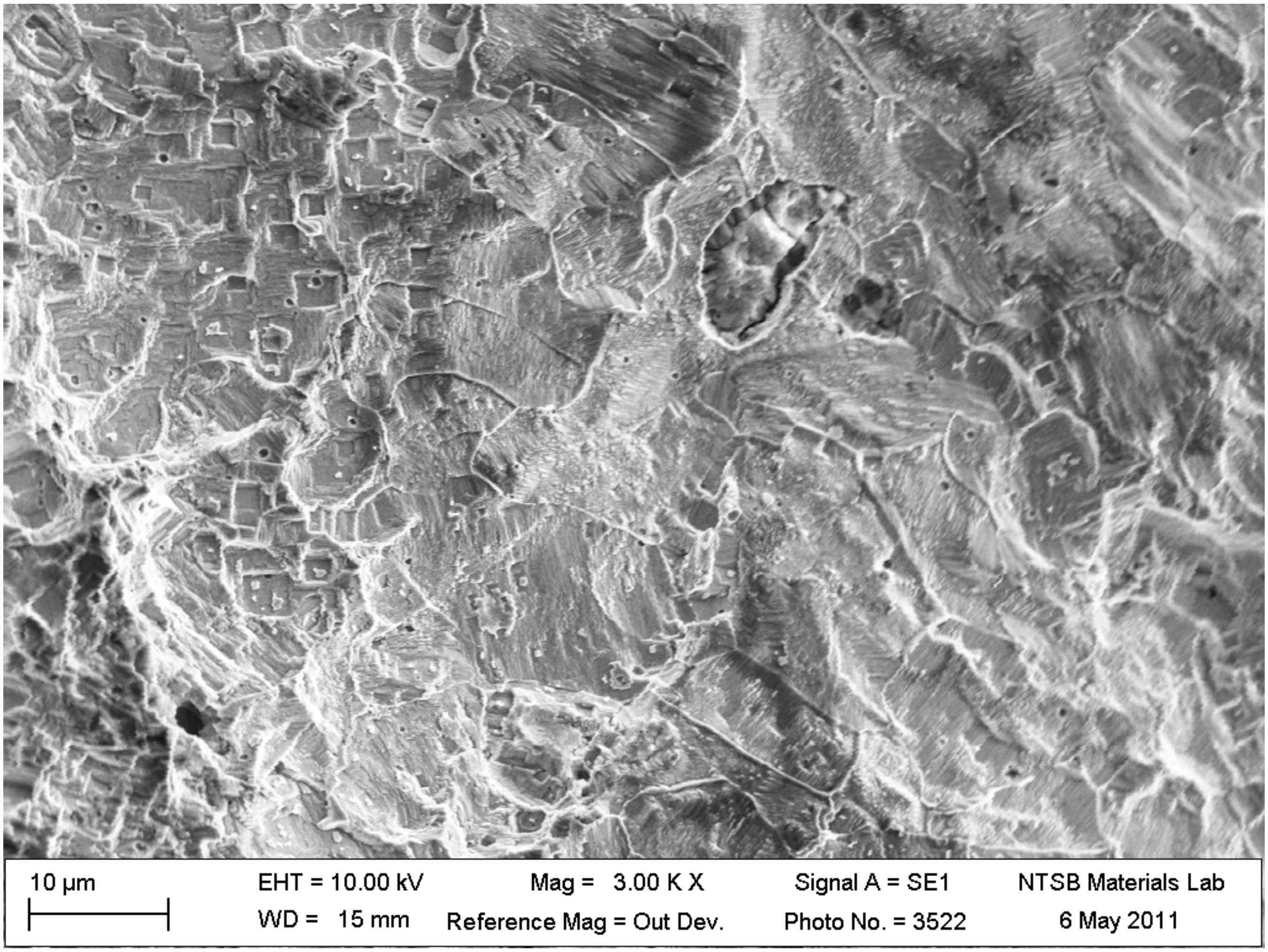

Figure 22: Etch pits and step/terrace features consistent with corrosion on the P3 CW fracture surface.

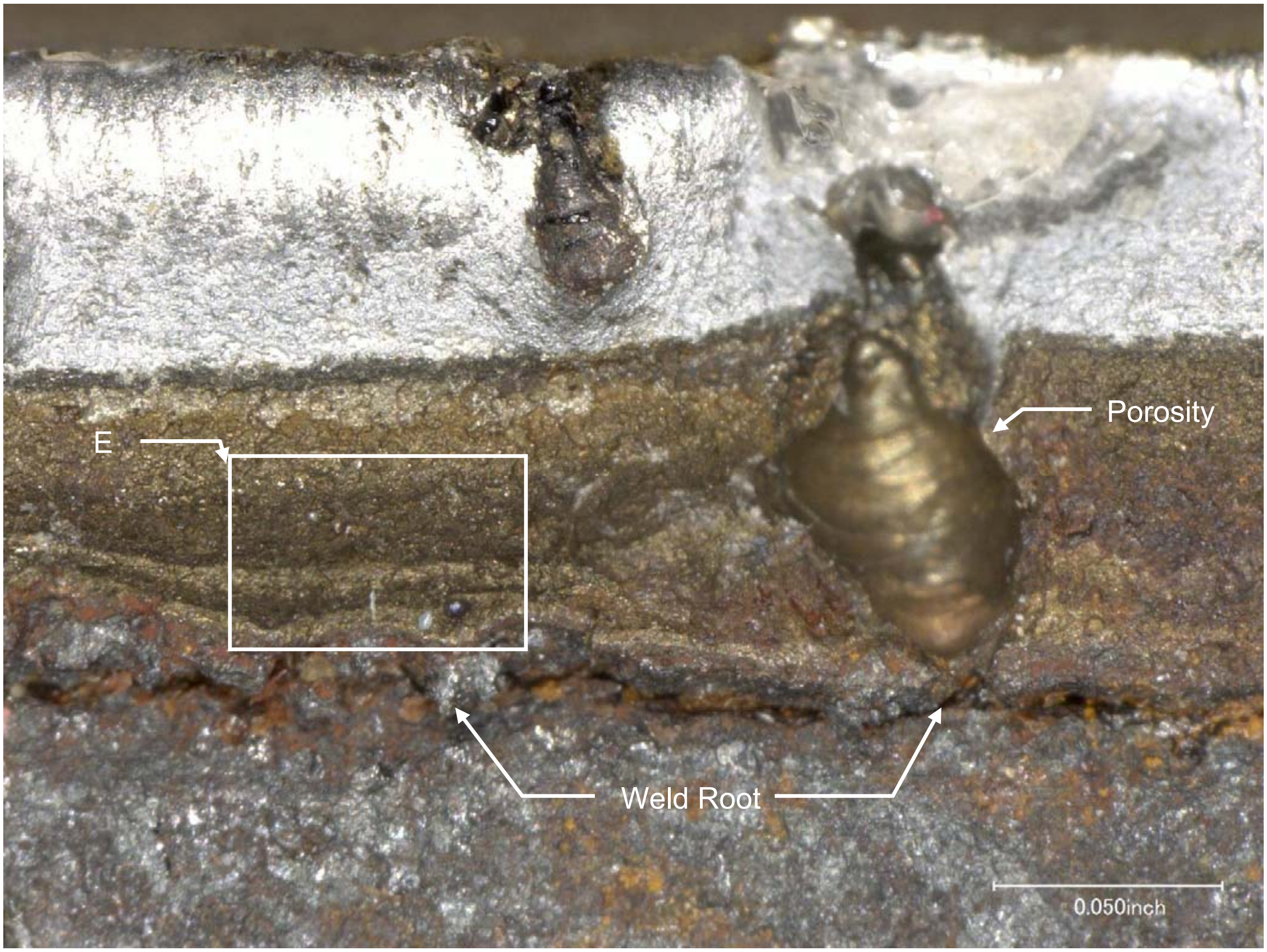

Figure 23: Higher magnification view of the region labeled D in Figure 20. Alternating light- and dark-colored bands were observed in the ductile fracture region. The region labeled E was examined by SEM, as shown in Figure 24.

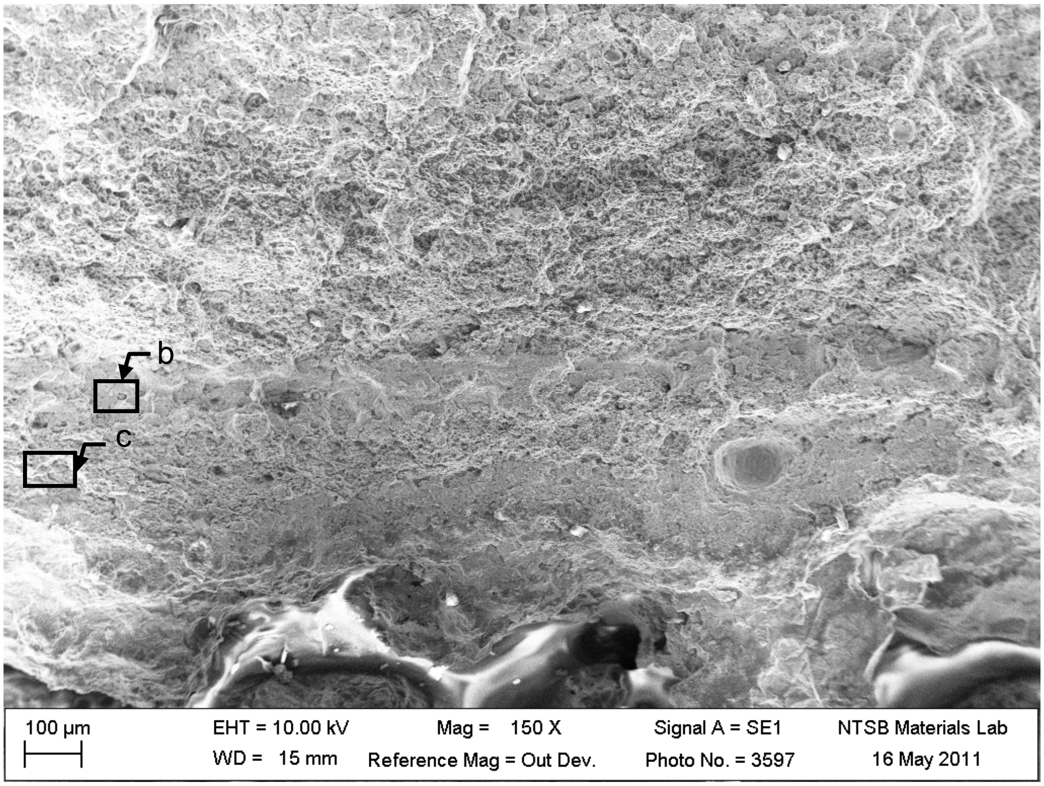

a)

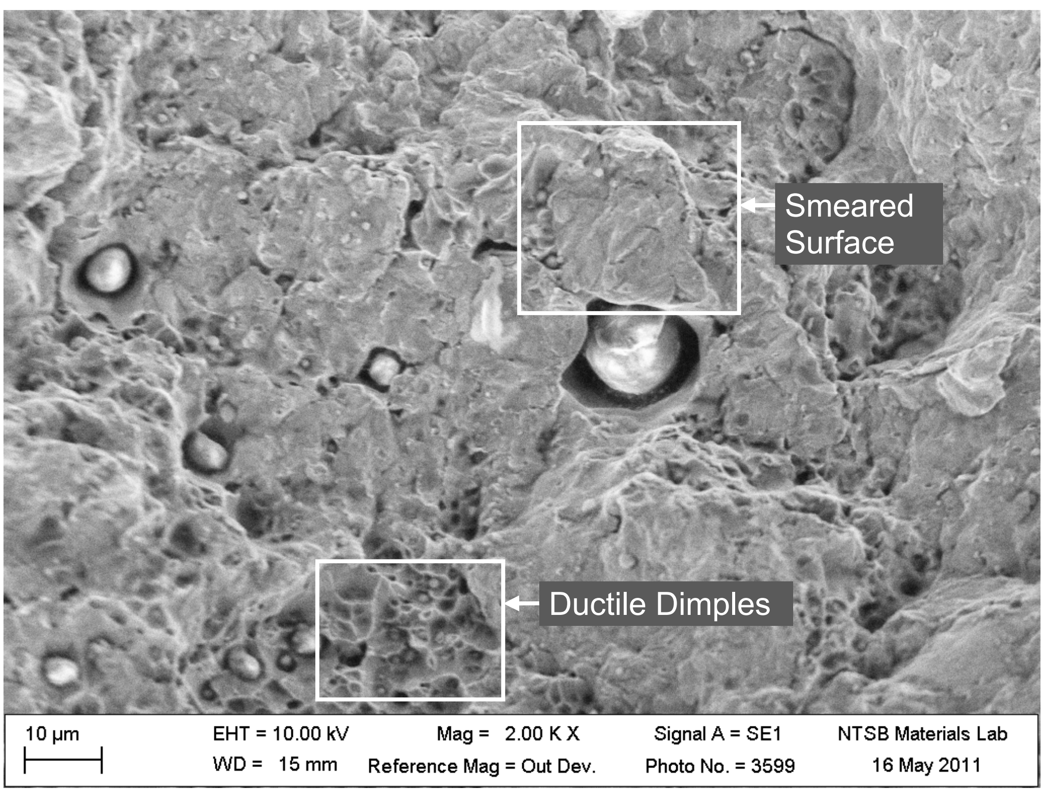

b)

Figure 24: a) SEM micrograph of the region labeled E in Figure 23; b) higher magnification image from the region indicated in part a). The fracture surface in the light-colored region was smeared with occasional dimples.

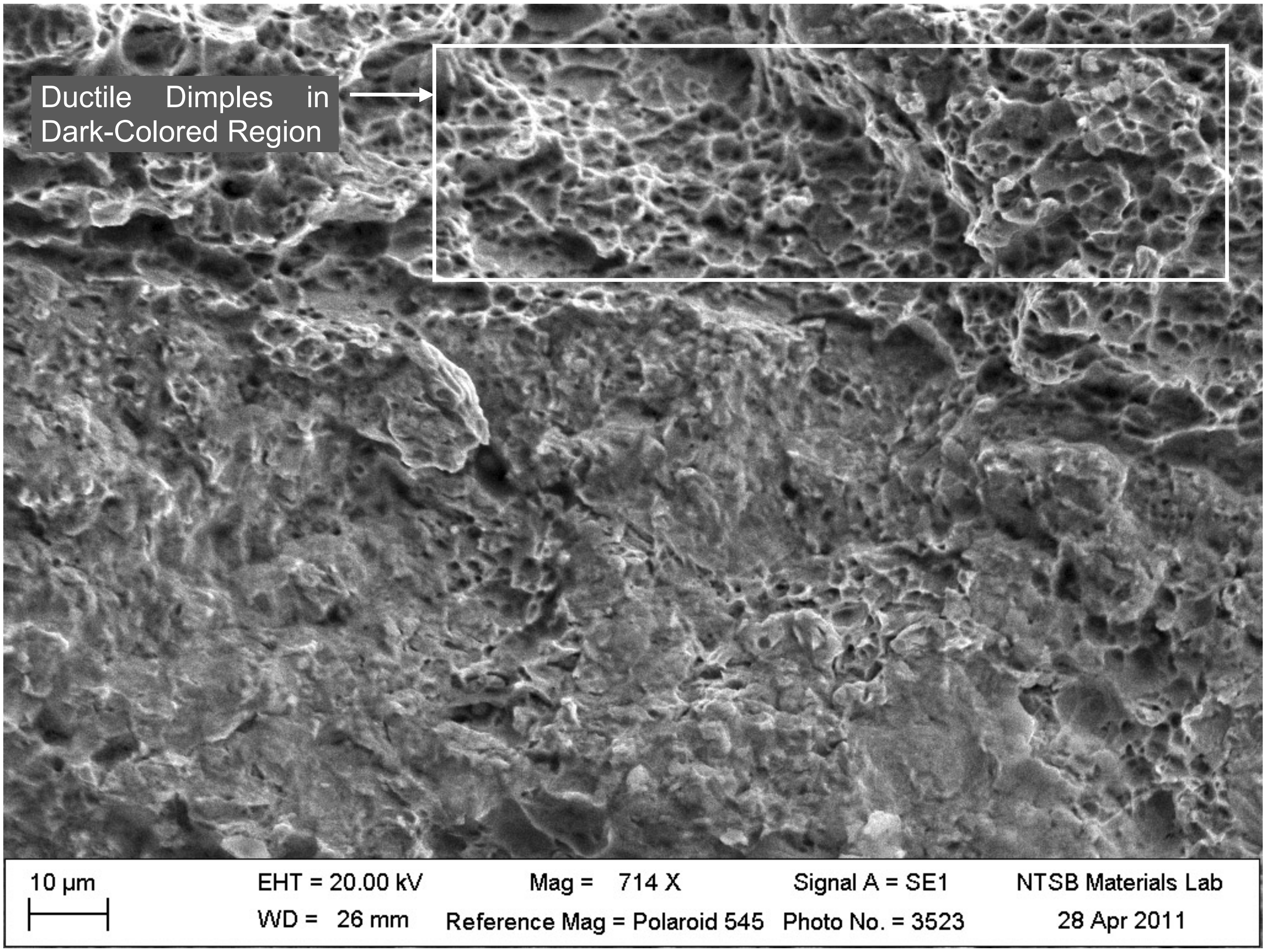

Figure 24 (cont.): c) the fracture surface in the dark-colored region consisted solely of ductile dimples.

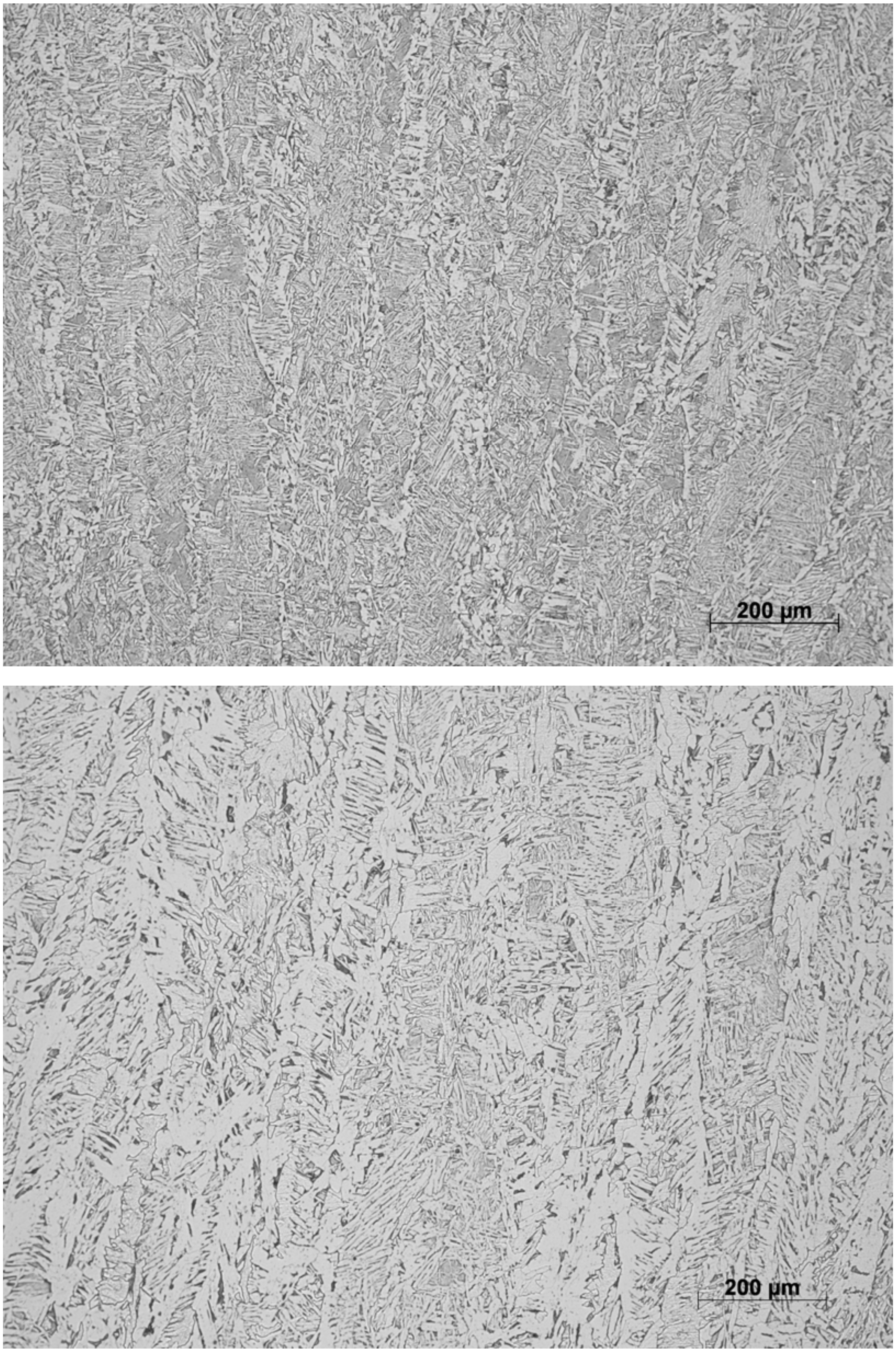

a)
b)

Figure 25: Micrographs of representative weld microstructure on cross sections from; a) LS longitudinal seam; b) P1 longitudinal seam. The micrographs were 100X original magnification. The sample was etched using a solution of 2% nitric acid in ethanol.

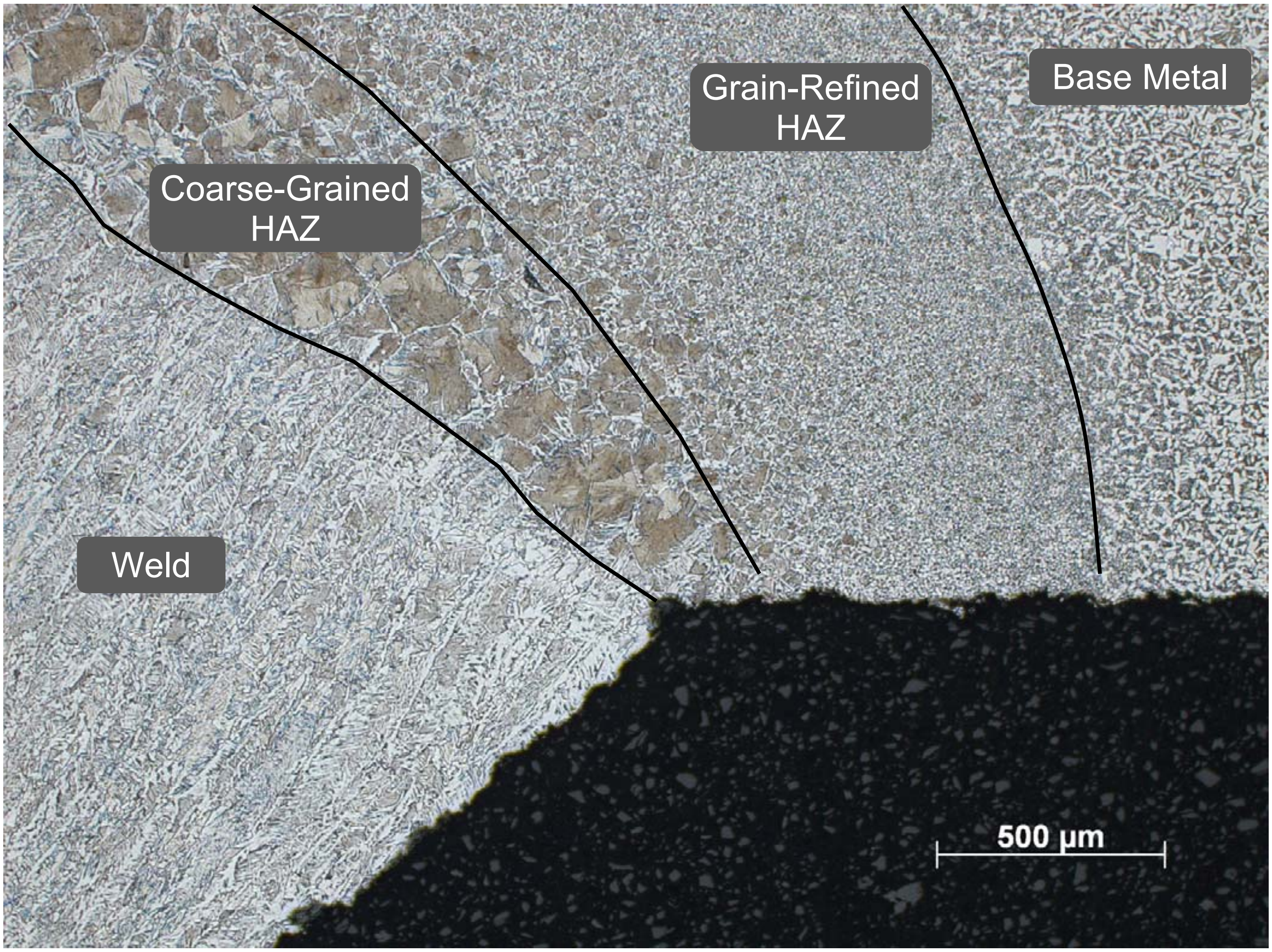

Figure 26: Micrograph of the LN longitudinal seam cross section showing weld, coarse-grained heat-affected zone (HAZ), grain-refined HAZ, and base metal regions examined by microhardness. Lines are superimposed on the micrograph to demarcate the various zones.

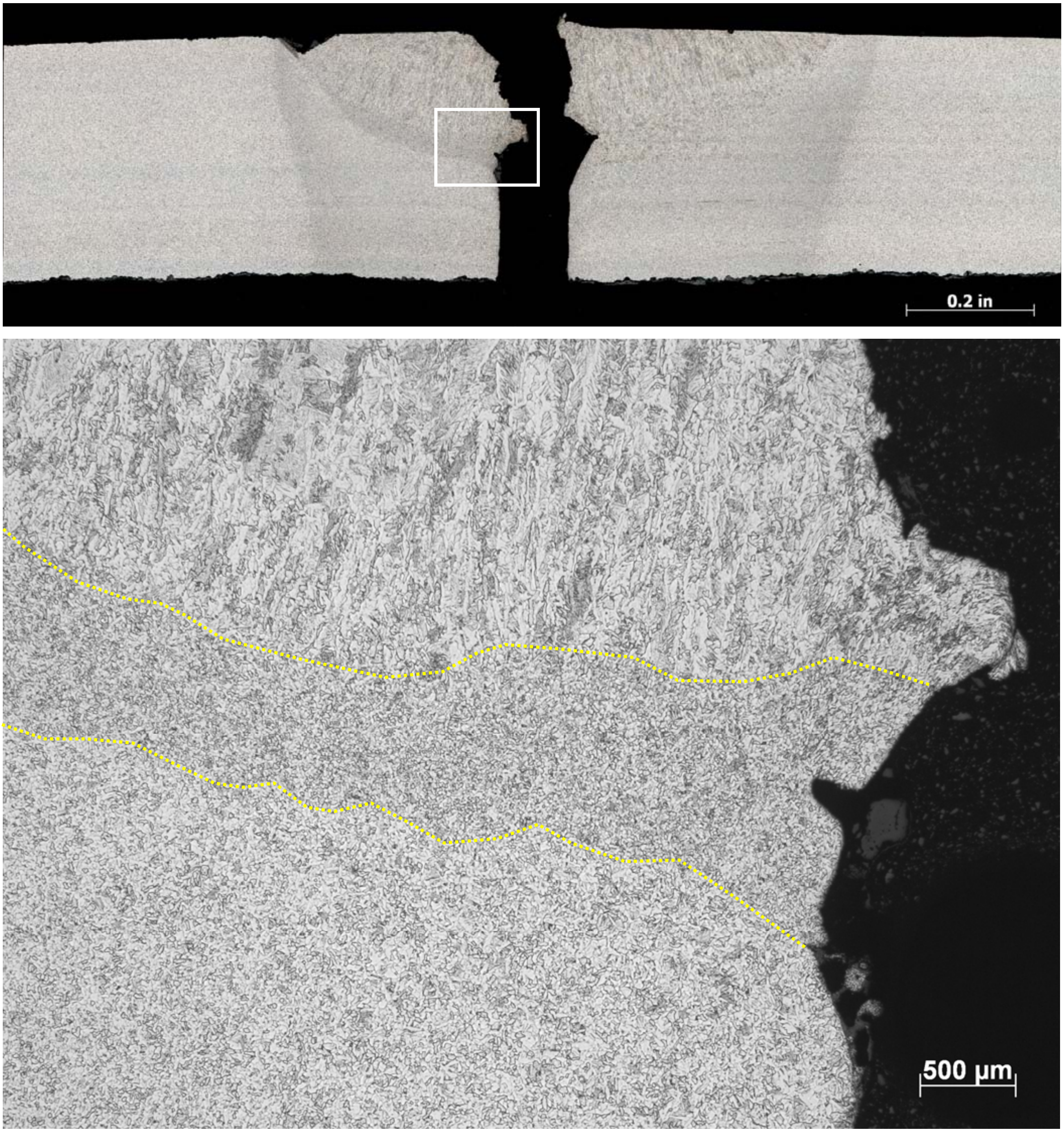

Figure 27: One side of the P2 longitudinal seam did not exhibit a coarse-grained HAZ at the base of the weld but, instead, a highly grain-refined region, consistent with the remnants of a previous welding pass. The region indicated by the rectangle in the top image is shown in greater detail in the bottom image. The grain-refined region is bound by two yellow-dashed lines.

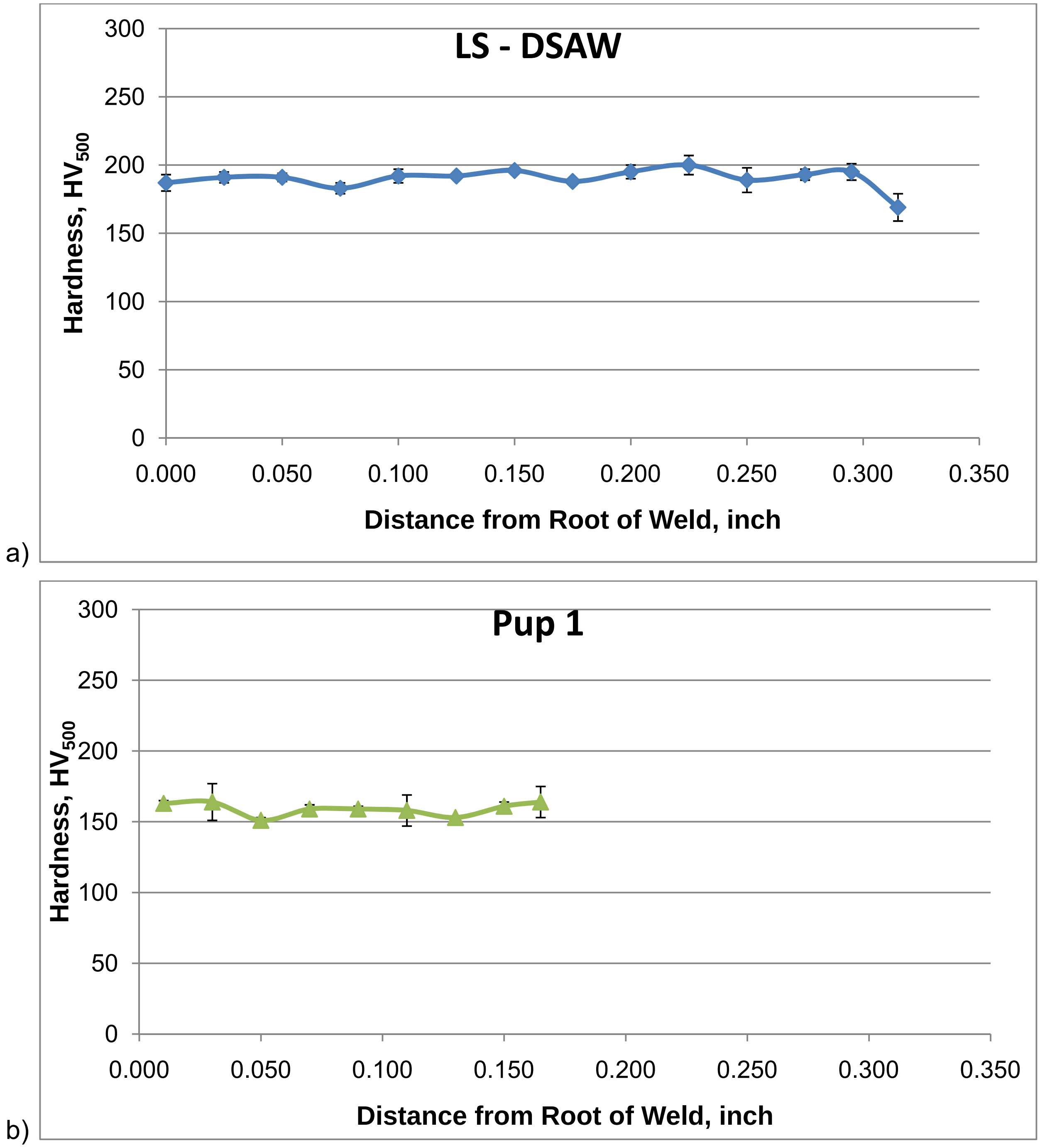

Figure 28: Vickers hardness profiles for a) LS and b) P1.

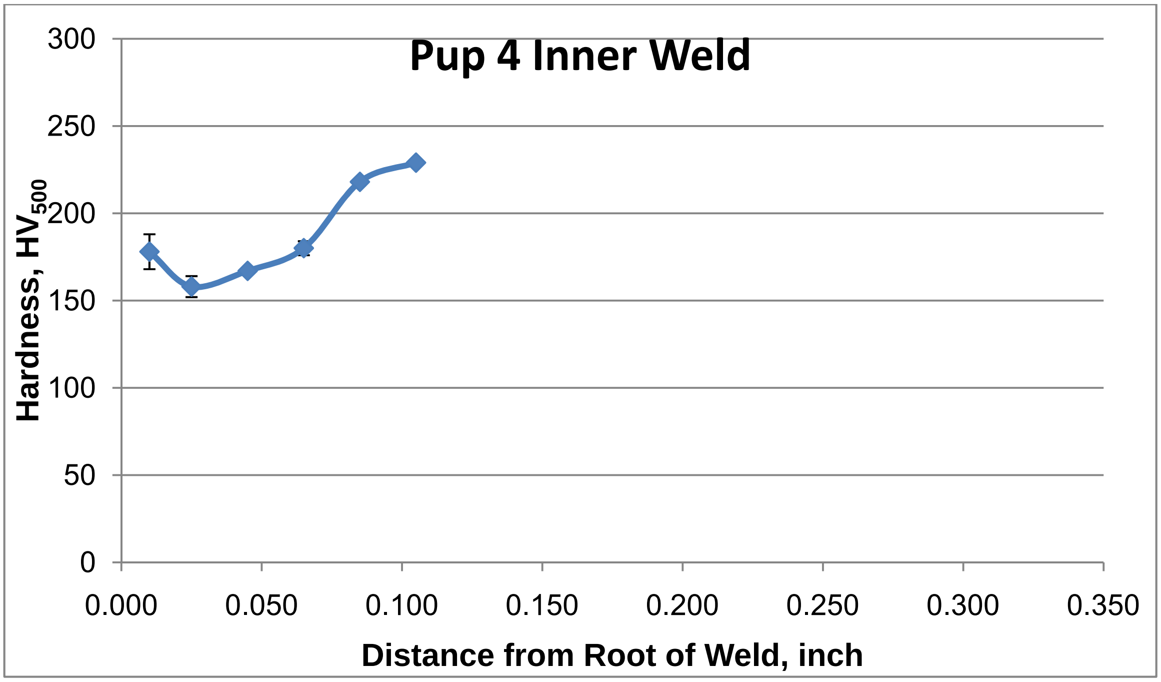

c)

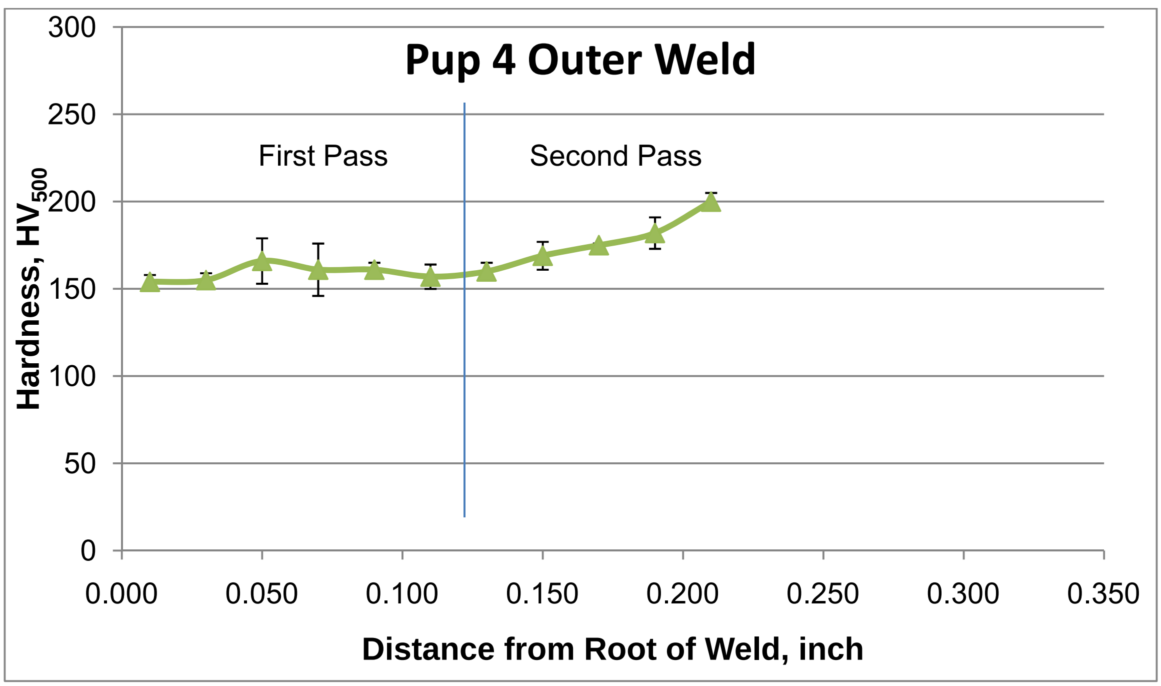

d)

Figure 28 (cont.): Vickers hardness profiles for c) inner weld on P4 and d) outer weld on P4.

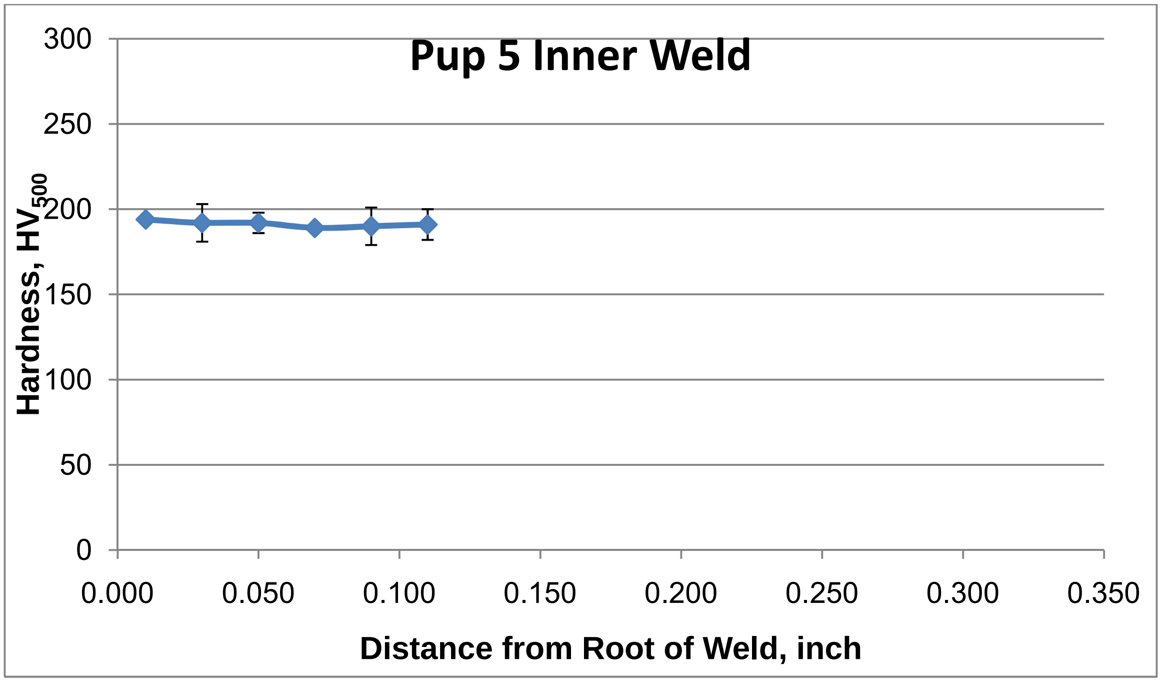

e)

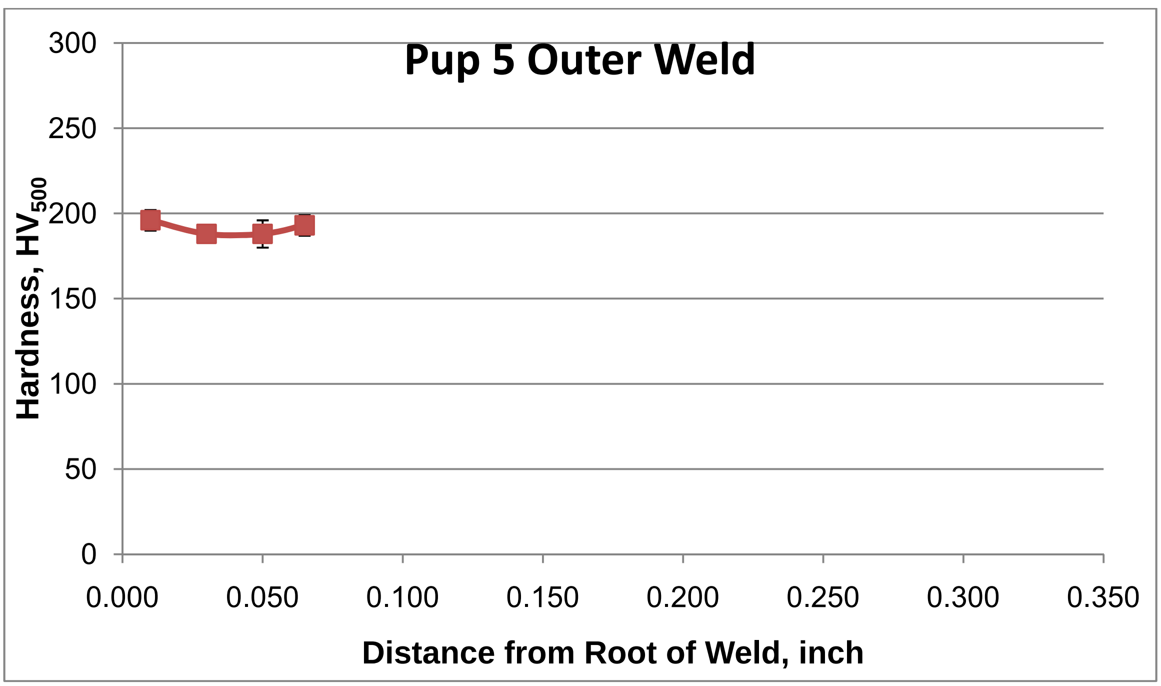

f)

Figure 28 (cont.): Vickers hardness profiles for e) inner weld on P5 and f) outer weld on P5.

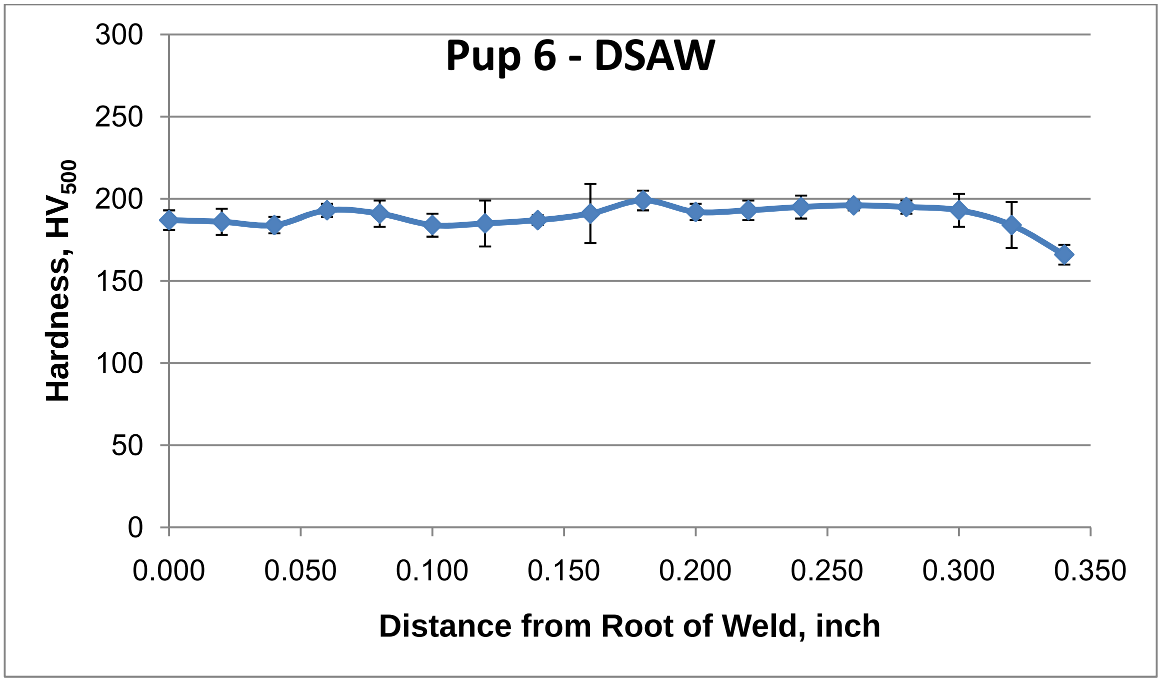

g)

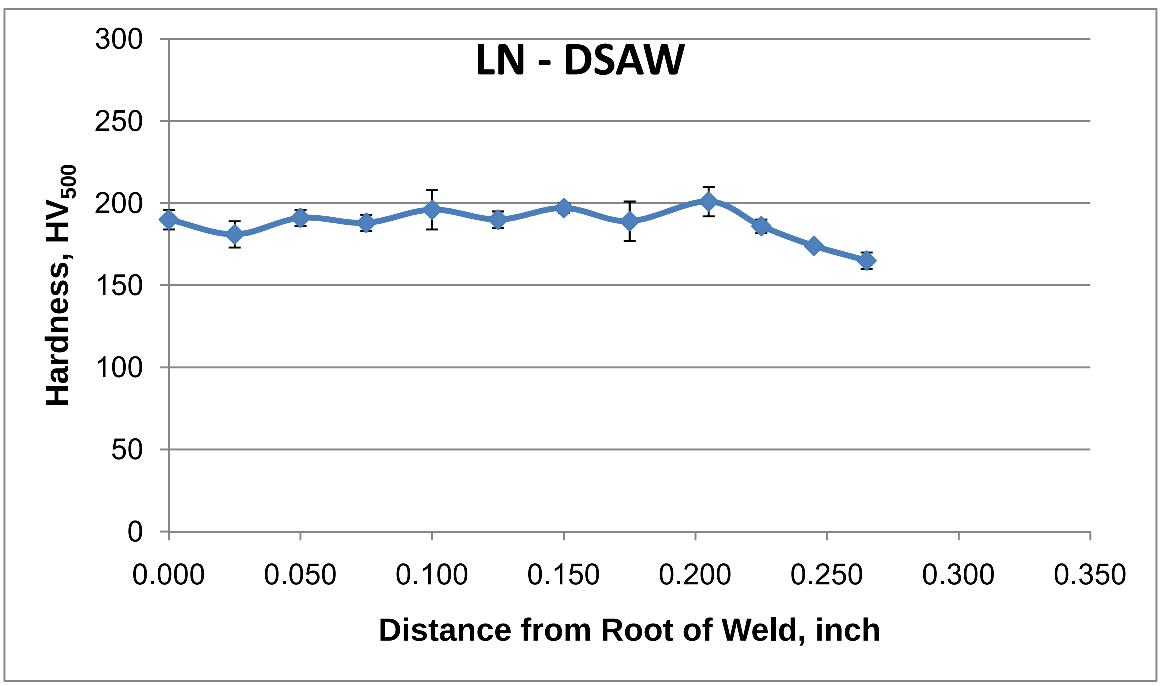

h)

Figure 28 (cont.): Vickers hardness profiles for g) P6 and h) LN.

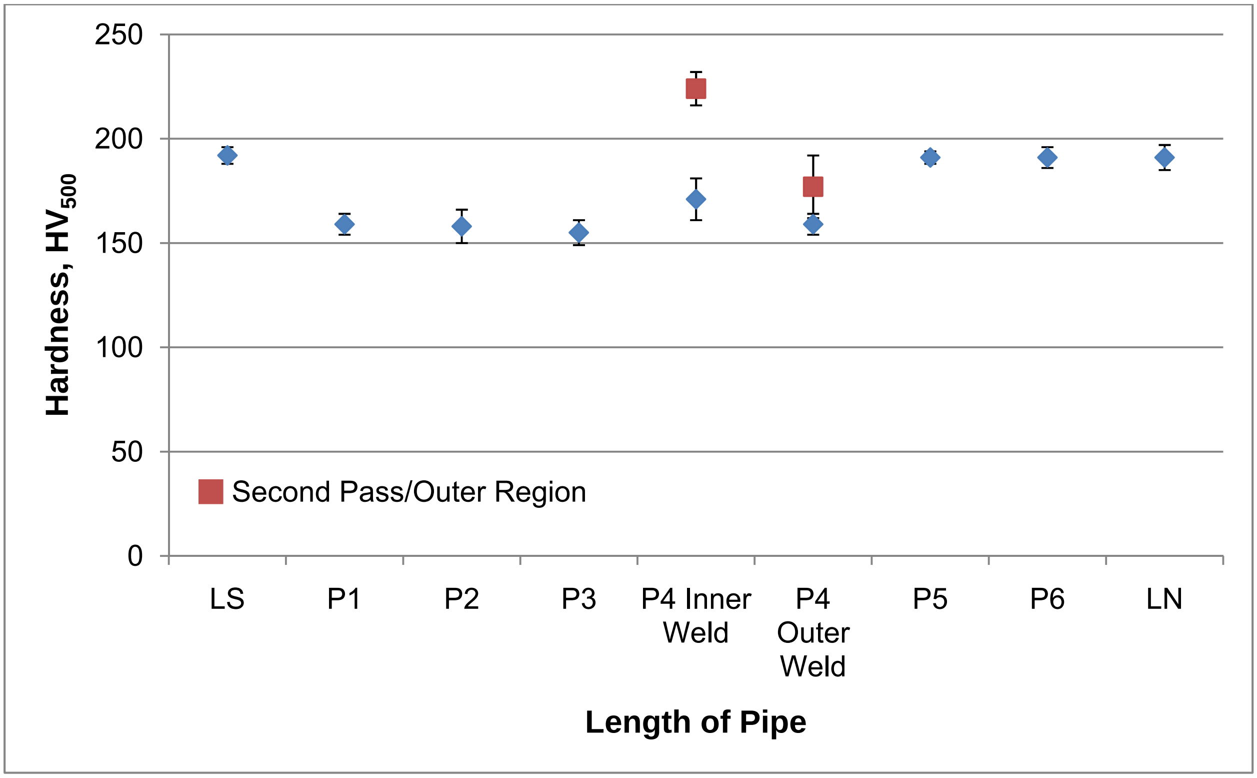

Figure 29: Comparison of the Vickers hardness values for each length of pipe.

a)
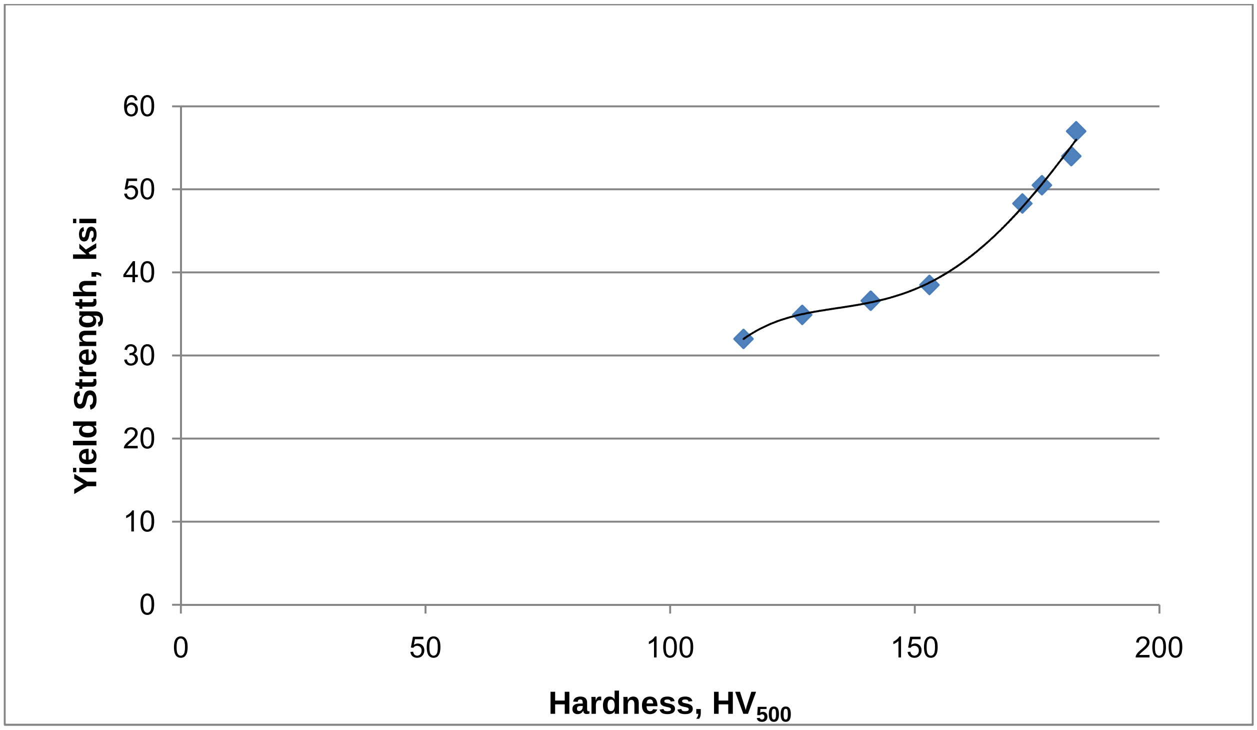

b)
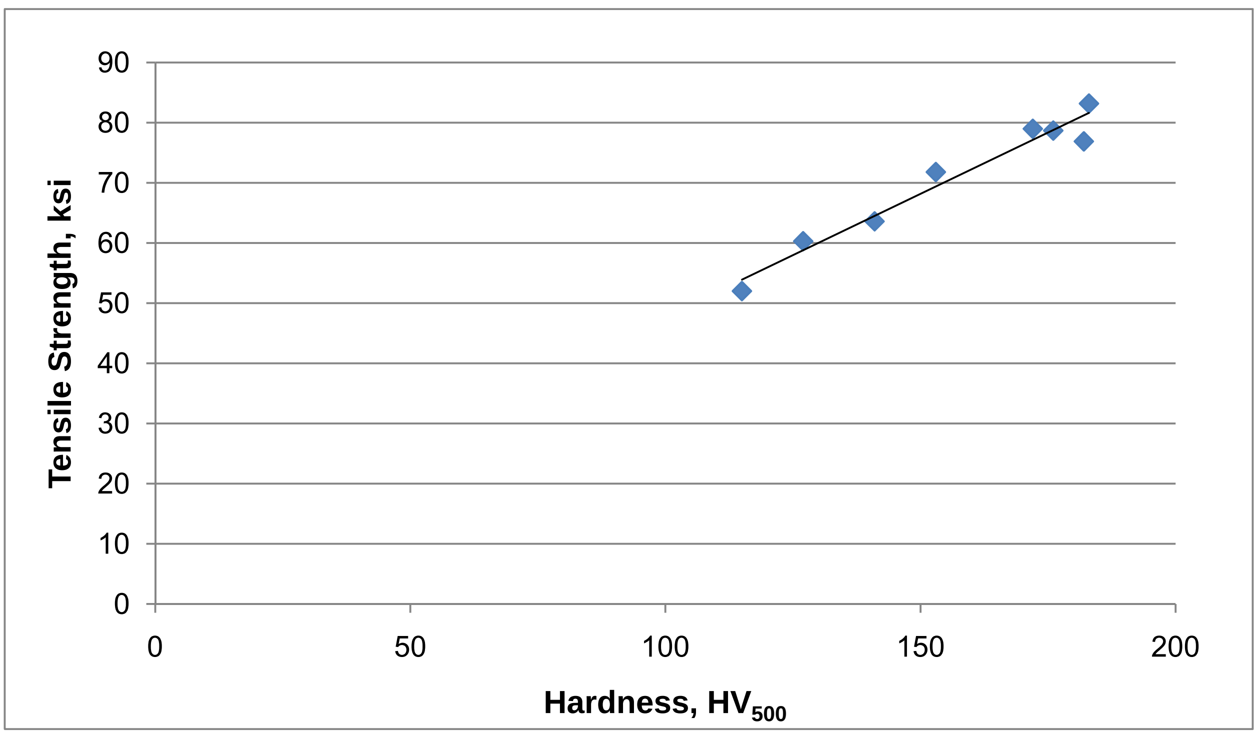

Figure 30: Correlation between base metal Vickers hardness numbers and; a) yield strength; b) tensile strength.

APPENDIX A: WALL THICKNESS MEAUREMENTS AT THE PUP 1 LONGITUDINAL SEAM INITIATION SITE

Table A-1: Wall thickness measurements at the P1 longitudinal seam initiation site measured on Figure 2. The data are presented graphically in Figure 6.

Longitudinal Distance, inch	Wall Thickness, inch	(Wall Thickness) - (Overstress), inch	(Wall Thickness) - (Overstress + Fatigue), inch
0.00	0.151	0.151	0.151
0.05	0.163	0.163	0.119
0.10	0.163	0.137	0.101
0.15	0.163	0.141	0.102
0.20	0.165	0.146	0.104
0.30	0.170	0.123	0.091
0.40	0.173	0.118	0.086
0.50	0.164	0.099	0.084
0.60	0.169	0.107	0.098
0.70	0.164	0.112	0.099
0.80	0.170	0.109	0.098
0.90	0.163	0.089	0.081
1.00	0.180	0.076	0.069
1.10	0.180	0.066	0.061
1.20	0.180	0.071	0.066
1.30	0.169	0.089	0.080
1.40	0.170	0.101	0.086
1.50	0.165	0.103	0.093
1.60	0.168	0.099	0.086
1.70	0.160	0.108	0.096
1.80	0.153	0.118	0.100
1.90	0.154	0.110	0.098
2.00	0.156	0.118	0.104
2.10	0.157	0.124	0.108
2.20	0.158	0.118	0.111
2.30	0.161	0.161	0.133
2.40	0.158	0.158	0.158

APPENDIX B: LONGITUDINAL SEAM WELD MEASUREMENTS FOR PUPS 2 AND 3

Table B-1: Wall thickness, weld depth, and unwelded depth data measured at regular intervals along the P2 longitudinal seam starting near girth weld C2 at the upstream end.

Position from Upstream End, inch	Wall Thickness, inch	Welded Depth, inch	Unwelded Depth, inch	Percent of Seam Welded
4.5	0.369	0.241	0.128	65.3
8.5	0.373	0.212	0.161	56.8
12.5	0.378	0.231	0.147	61.1
16.5	0.364	0.210	0.154	57.7
20.5	0.372	0.208	0.164	55.9
24.5	0.366	0.142	0.224	38.8
28.5	0.358	0.136	0.222	38.0
32.5	0.367	0.197	0.170	53.7
36.5	0.370	0.220	0.150	59.5
40.5	0.367	0.208	0.159	56.7

Table B-2: Wall thickness, weld depth, and unwelded depth data measured at regular intervals along the P3 longitudinal seam starting near girth weld C3 at the upstream end.

Position from Upstream End, inch	Wall Thickness, inch	Welded Depth, inch	Unwelded Depth, inch	Percent of Seam Welded
5.0	0.359	0.158	0.201	44.0
9.0	0.350	0.174	0.176	49.7
13.0	0.358	0.166	0.192	46.4
17.0	0.344	0.177	0.167	51.5
21.0	0.343	0.156	0.187	45.5
25.0	0.358	0.155	0.203	43.3
29.0	0.352	0.180	0.172	51.1
33.0	0.353	0.142	0.211	40.2
37.0	0.357	0.149	0.208	41.7
41.0	0.353	0.146	0.207	41.4

APPENDIX C: MICROHARDNESS DATA

Table C-1: Vickers hardness profiles for the LS longitudinal seam. The root of the inner seam weld started at 0.325 inch.

Distance from Cap of Inner Diameter Weld, inch	Profile 1, HV_{500}	Profile 2, HV_{500}	Profile 3, HV_{500}
0.010	158	177	173
0.030	198	198	188
0.050	197	189	193
0.075	179	195	194
0.100	199	194	208
0.125	191	194	201
0.150	190	188	187
0.175	195	197	197
0.200	191	193	192
0.225	187	197	191
0.250	182	187	180
0.275	189	195	189
0.300	189	189	196
0.325	193	181	186
0.350	177	175	176
0.375	172	167	180
0.400	168	175	173
0.425	176	172	174
0.450	176	170	173
0.475	174	176	173
0.500	176	176	175
0.525	180	181	182
0.550	181	174	175
0.575	194	192	172

Table C-2: Vickers hardness profiles for the P1 longitudinal seam.

Distance from Root of Weld, inch	Profile 1, HV_{500}	Profile 2, HV_{500}	Profile 3, HV_{500}
0.010	161	165	163
0.030	154	179	164
0.050	149	151	151
0.070	158	157	159
0.090	158	159	159
0.110	161	146	158
0.130	153	154	153
0.150	159	164	161
0.165	175	164	164

Table C-3: Vickers hardness profiles for the P2 longitudinal seam. The seam was fractured through the weld. Four microhardness profiles were acquired perpendicular to the seam, two on either side of the fracture.

Distance from Fracture, inch	Profile 1, HV_{500}	Profile 2, HV_{500}	Profile 3, HV_{500}	Profile 4, HV_{500}
0.015	220	198	178	205
0.035	229	178	183	195
0.055	203	181	174	178
0.075	182	176	179	169
0.095	192	169	152	164
0.115	171	180	179	151
0.135	150	152	145	149
0.155	150	146	164	149
0.175	176	151	158	155
0.195	161	149	157	169
0.215	165	155	—	153
0.235	165	165	—	160
0.255	161	—	—	161
0.275	152	—	—	160
0.295	173	—	—	—
0.315	166	—	—	—

Table C-4: Vickers hardness profiles for the P3 longitudinal seam. The seam was fractured through the weld. Four microhardness profiles were acquired perpendicular to the seam, two on either side of the fracture.

Distance from Fracture, inch	Profile 1, HV_{500}	Profile 2, HV_{500}	Profile 3, HV_{500}	Profile 4, HV_{500}
0.015	184	181	216	194
0.035	157	161	199	197
0.055	152	153	166	186
0.075	152	162	165	158
0.095	145	147	150	157
0.115	152	155	154	148
0.135	164	—	158	159
0.155	150	—	152	165
0.175	—	—	160	147
0.195	—	—	—	154

Table C-5: Vickers hardness profiles for the P4 longitudinal seam.

Inner Weld			
Distance from Root of Weld, inch	**Profile 1, HV_{500}**	**Profile 2, HV_{500}**	**Profile 3, HV_{500}**
0.010	184	183	166
0.025	158	152	164
0.045	168	167	166
0.065	184	180	176
0.085	220	217	216
0.105	229	228	230
Outer Weld			
Distance from Root of Weld, inch	**Profile 1, HV_{500}**	**Profile 2, HV_{500}**	**Profile 3, HV_{500}**
0.010	154	150	157
0.030	158	151	155
0.050	163	155	180
0.070	155	150	178
0.090	157	164	163
0.110	151	165	156
0.130	162	154	163
0.150	175	160	172
0.170	174	175	175
0.190	192	177	176
0.210	195	205	201

Table C-6: Vickers hardness profiles for the P5 longitudinal seam.

Inner Weld			
Distance from Root of Weld, inch	**Profile 1, HV_{500}**	**Profile 2, HV_{500}**	**Profile 3, HV_{500}**
0.010	—	194	193
0.030	184	205	187
0.050	188	189	198
0.070	187	188	191
0.090	203	183	184
0.110	201	184	187
Outer Weld			
Distance from Root of Weld, inch	**Profile 1, HV_{500}**	**Profile 2, HV_{500}**	**Profile 3, HV_{500}**
0.010	189	197	201
0.030	193	189	183
0.050	197	182	184
0.065	196	198	186

Table C-7: Vickers hardness profiles for the P6 longitudinal seam. The root of the inner seam weld started at 0.350 inch.

Distance from Cap of Inner Diameter Weld, inch	Profile 1, HV_{500}	Profile 2, HV_{500}	Profile 3, HV_{500}
0.010	171	167	159
0.030	200	176	175
0.050	194	202	183
0.070	198	190	197
0.090	198	197	192
0.110	188	195	201
0.130	200	188	191
0.150	194	187	196
0.170	205	193	199
0.190	211	179	182
0.210	187	185	190
0.230	200	181	173
0.250	189	176	188
0.270	199	183	191
0.290	197	189	192
0.310	180	182	189
0.330	185	178	194
0.350	193	182	185
0.370	183	175	175
0.390	193	188	175
0.410	186	179	179
0.430	185	173	173
0.450	187	183	171
0.470	183	171	181
0.490	175	175	167
0.510	187	170	175
0.530	185	180	173
0.550	188	154	166
0.570	—	172	181

Table C-8: Vickers hardness profiles for the LN longitudinal seam. The root of the inner seam weld started at 0.275 inch.

Distance from Cap of Inner Diameter Weld, inch	Profile 1, HV_{500}	Profile 2, HV_{500}	Profile 3, HV_{500}
0.010	165	160	170
0.030	172	173	176
0.050	185	190	183
0.070	207	191	205
0.100	202	180	184
0.125	198	193	199
0.150	192	185	194
0.175	208	185	196
0.200	186	184	194
0.225	196	191	187
0.250	182	173	188
0.275	197	186	187
0.300	186	178	188
0.325	186	184	180
0.350	180	179	175
0.375	184	182	180
0.400	194	176	174
0.425	190	181	184
0.450	179	185	178
0.475	196	179	191
0.500	203	197	187

Table C-9: Coarse-grained HAZ Vickers hardness data (HV_{500}).

LS	P1	P2	P3	P4	P5	P6	LN
216	214	151	146	213	226	187	212
203	179	157	149	202	240	202	202
212	197	134	151	195	219	196	209
204	176	157	158	193	214	189	221
204	189	156	165	217	229	208	210
191	208	144	159	198	230	201	202
191	221	161	208	197	256	195	228
219	199	145	188	195	250	208	201
222	177	165	167	205	228	202	208
207	193	—	179	204	229	211	214
222	223	—	169	211	234	207	210
203	194	—	180	193	222	207	192
—	—	—	172	184	—	—	—
—	—	—	204	199	—	—	—
—	—	—	—	210	—	—	—
—	—	—	—	197	—	—	—
—	—	—	—	211	—	—	—

Table C-10: Grain-refined HAZ Vickers hardness data (HV_{500}).

LS	P1	P2	P3	P4	P5	P6	LN
187	158	119	131	181	188	166	177
184	154	115	135	187	190	176	189
187	143	120	133	183	188	183	192
179	149	107	131	176	198	181	180
184	147	108	153	200	191	171	187
182	152	118	133	176	197	178	207
194	145	111	136	189	183	169	182
183	146	117	136	175	188	178	183
189	143	113	133	179	182	179	194
184	144	109	141	187	193	164	194
182	142	109	139	193	191	173	186
189	142	117	136	195	200	179	184
—	—	—	134	—	—	—	—
—	—	—	132	—	—	—	—
—	—	—	131	—	—	—	—
—	—	—	134	—	—	—	—

Table C-11: Base metal Vickers hardness data (HV_{500}).

LS	P1	P2	P3	P4	P5	P6	LN
189	133	112	121	186	152	175	190
175	145	117	136	171	149	164	176
191	146	126	130	176	149	183	194
177	145	115	128	170	151	181	173
184	136	115	133	164	147	172	175
190	149	121	121	173	150	174	181
192	138	104	122	162	175	182	200
180	139	123	127	172	157	175	186
181	144	114	119	180	153	177	186
182	134	109	125	166	153	169	189
197	154	116	131	175	176	164	180
181	135	108	126	165	152	175	188
186	144	111	135	179	149	170	174
184	137	112	130	169	141	181	169
162	145	120	128	160	146	183	184
181	139	113	133	176	144	179	186
182	136	115	123	178	145	174	170
165	141	121	133	180	152	197	172
198	139	109	126	175	158	175	179
193	145	113	121	169	152	181	181
175	—	—	—	164	146	166	181
183	—	—	—	167	160	167	193
—	—	—	—	—	155	—	181
—	—	—	—	—	168	—	171